UNIVERSITÀ DEGLI STUDI DELLA TUSCIA
DIPARTIMENTO DI SCIENZE ECOLOGICHE E BIOLOGICHE

ELIXIR workshop on:
Metabolomics and Integrative omics: from data production to analysis

Bari, 28-29 April 2022

Anna Maria Timperio https://www.researchgate.net/profile/Anna-Timperiohttps://orcid.org/0000-0001-8457-042X

Three different examples:

UNIVERSITÀ DEGLI STUDI DELLA TUSCIA
DIPARTIMENTO DI SCIENZE ECOLOGICHE E BIOLOGICHE

1 **Specific adaptations are selected in opposite sun exposed Antarctic cryptoendolithic communities as revealed by untargeted metabolomics.**

2 **Urine Metabolome during Parturition.**

3 **Plastic and Placenta: Identification of polyethylene glycol (PEG) compounds in the human placenta by HPLC-MS/MS system.**

Specific adaptations are selected in opposite sun exposed Antarctic cryptoendolithic communities as revealed by untargeted metabolomics.

Coleine, C., Gevi, F., Fanelli, G., ...Timperio, A.M., Selbmann, L. *PLoS ONE*, 2020, 15(5)

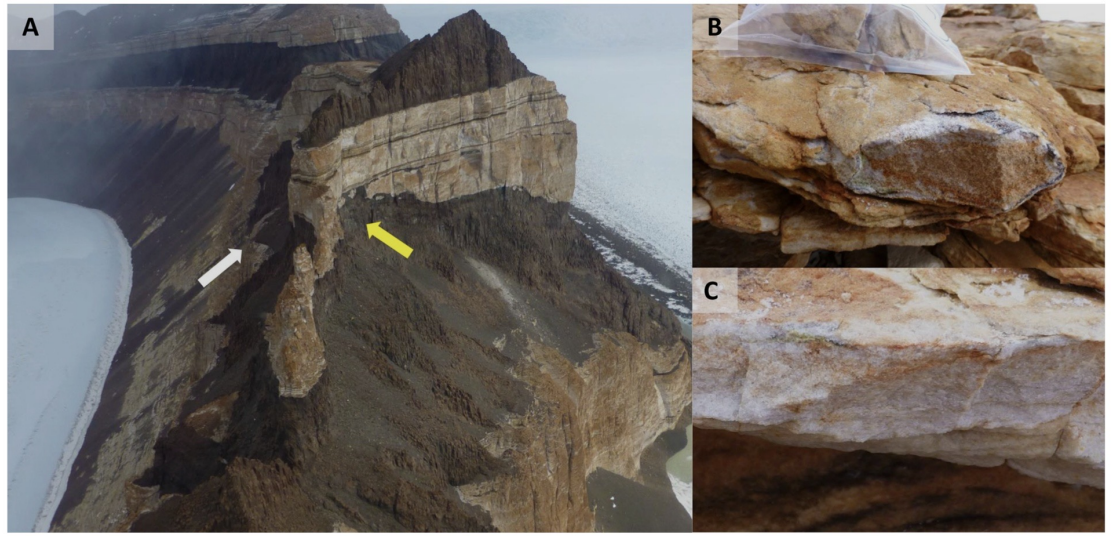

Fig 1. A) Finger Mt. landscape: the yellow arrow indicates the north exposed surface, while the white arrow indicates the south exposed surface; B) north exposed sandstone rock; C) south exposed sandstone rock.

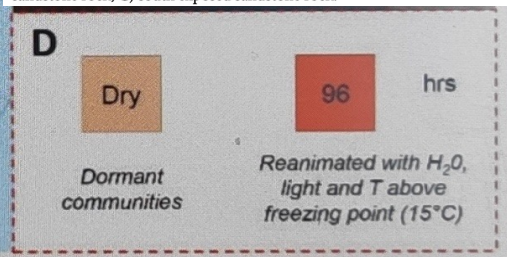

Figure 1. (A) Map of Antarctica. Red symbol indicates the study area, Finger Mt. (McMurdo Dry Valleys, Southern Victoria Land, Continental Antarctica); (B) Northern and (C) southern exposed rock surfaces; (D) outline of reactivation experiment. Credit by Italian National Antarctic Research Program (PNRA).

Endolithic microbial communities are found inside rocks

Excellent models to explore biotic and abiotic drivers of diversity, and responses under stress conditions, giving clues into the limit of life on Earth, and also for exploring the possibility for life elsewhere in the Solar System (e.g., Mars).

Extreme climatic condition: drastic temperature fluctuations, water deficit, prolonged periods of desiccation, oligotrophy, and high salinity. as a Terrestrial Martian analogue.

SUMMARY:

UNIVERSITÀ DEGLI STUDI DELLA TUSCIA
DIPARTIMENTO DI SCIENZE ECOLOGICHE E BIOLOGICHE

Antarctic cryptoendolithic communities are self-supporting borderline ecosystems.

They live in the extreme conditions of the Antarctic desert accounted as the closest terrestrial Martian analogue

They need to develop survival strategies to address external conditions

Components of these communities are highly adapted extremophiles and extreme-tolerant microorganisms, among the most resistant known to date.

Using an untargeted metabolomics, we explored stress-response of communities spreading in two sites of the same location.

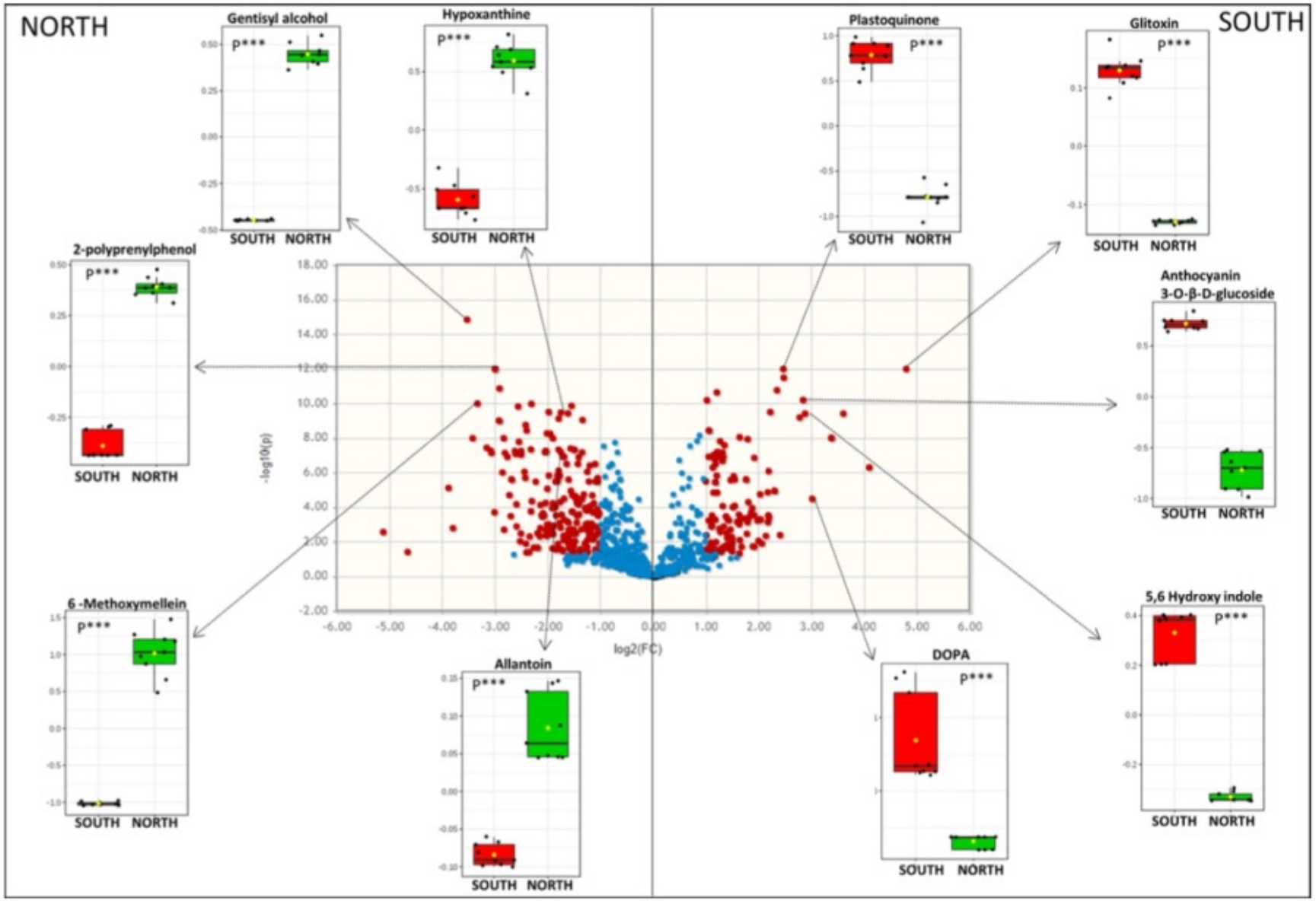

Fig 2. Volcano plot analysis of metabolic changes Finger Mt. north and Finger Mt. south. Each point on the volcano plot was based on both p-value and fold-change values, and in this study these two values were set at 0.05 and 2.0, respectively. The points which satisfy the condition $p < 0.05$ and fold change > 2.0 appear in red and are marker candidates, whereas the others appear in blue that are not significant. The potential biomarkers between experimental groups were annotated with their matched metabolite names. Bar plots show the original values (mean +/- SD). Differences were considered statistically significant at $^{*}p < 0.05$ further stratified to $^{**}p < 0.01$ and $^{***}p < 0.001$ respectively.

To validate our date we use multistatistical analysis and we applied an untargeted metabolomics analysis on six differently exposed rocks

The significant discriminating metabolites were identified using the Volcano plot analysis the univariate analysis **we identified significant accumulation of specific metabolites; most of them were north exposure, while few others were overexpressed in south exposed rocks.**

206 metabolites were significantly upregulated in Antarctic cryptoendolithic communities of rocks exposed to the north whereas 125 were significantly upregulated in the south exposed ones

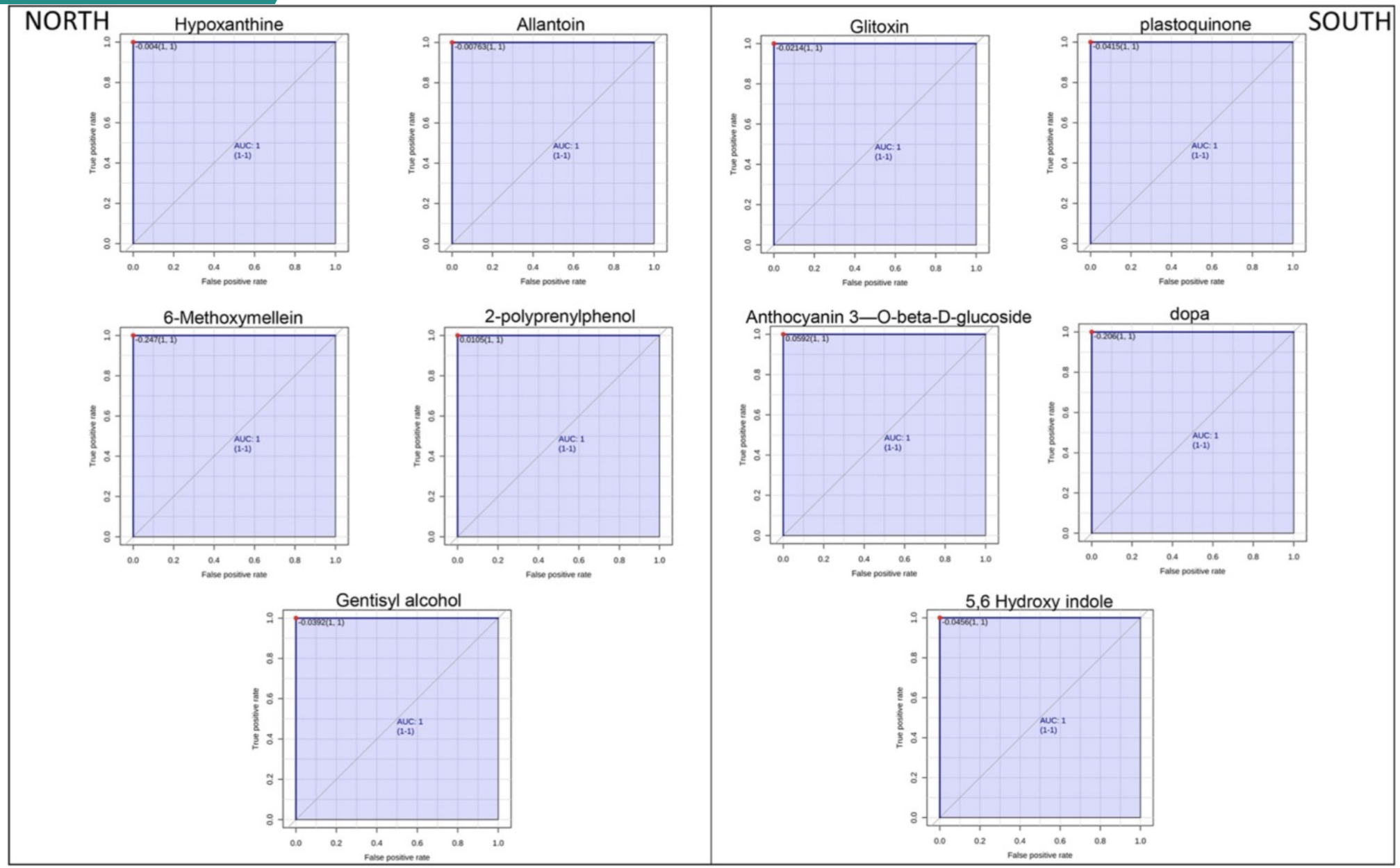

Fig 3. Area under the receiver-operating characteristic curves (AUROC) of the significant metabolite (with AUROC value > 0.9) identified 5 metabolites (Allantoin, Hypoxanthine, 6-Methoxymellein, 2-Polyprenylphenol and Lomefloxacin hydrochloride) as significantly elevated in Finger Mt. north samples and 5 metabolites (Gliotoxin, Plastoquinone, Anthocyanin 3-O-β-D-glucoside, 5–6 Dihydroxyindole and L-DOPA) significantly elevated in Finger Mt. south samples. They are candidate biomarkers with excellent value (AUC = 1; CI = 1–1).

We selected 10 metabolites from volcano plot and performed two-stage Receiver Operating Characteristic (ROC) analysis to test them as potential biomarkers.

Five significantly upregulated metabolites in the north-exposed communities (*we focus on allantoin that plays a crucial rolo on this comunitie*)

and **five metabolites increased significantly in those facing south (*Gliotoxin*, *Plastoquinone*, *Anthocyanin 3-O-β-D-glucoside*, *5–6 Dihydroxyindole* and *L-DOPA precursors of melanin*)**

Significant changes observed in the intermediates allantoin biosynthesis

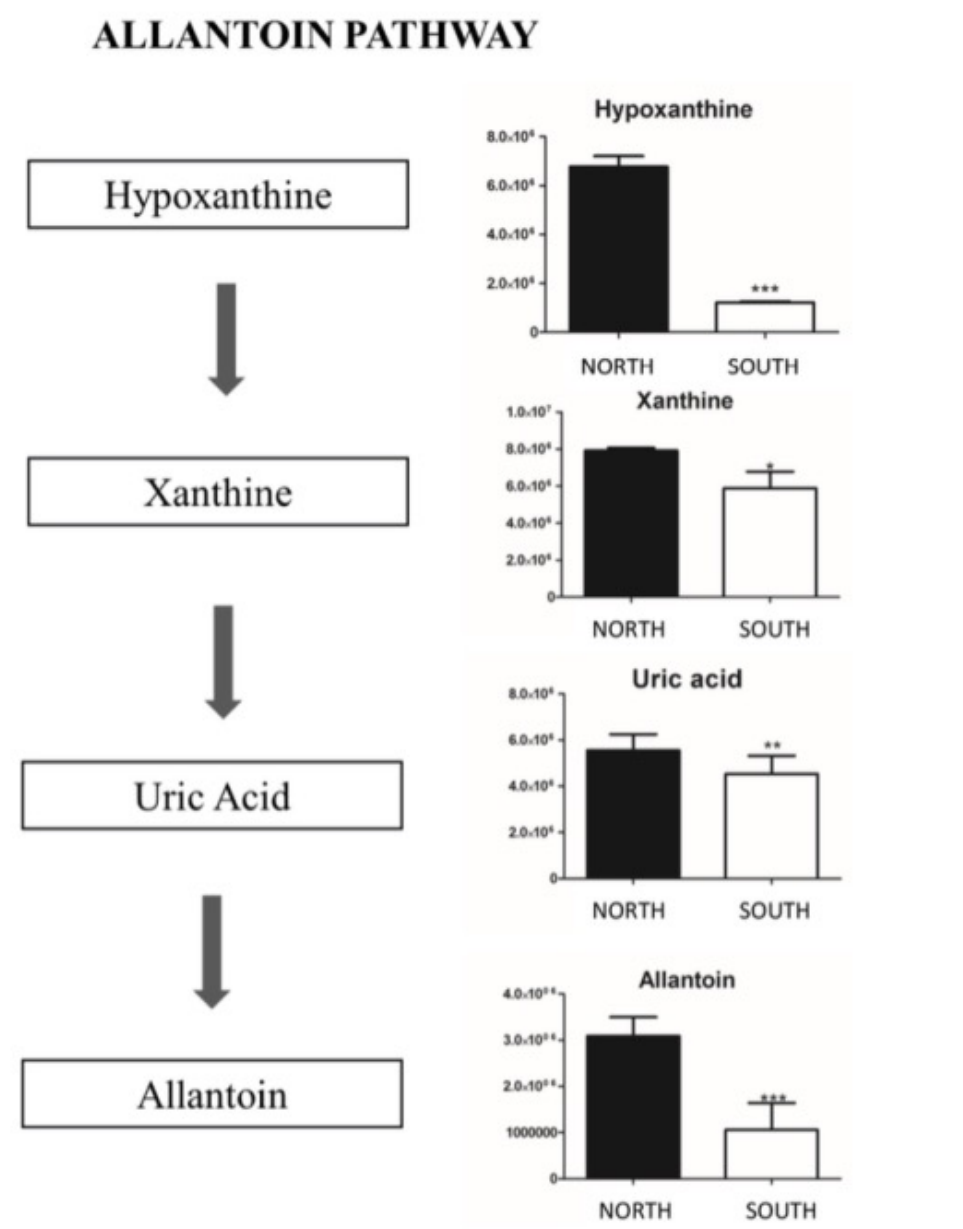

Fig 4. Allantoin pathway. Total amount of allantoin pathway intermediates appears to be increased in Finger Mt. north. Metabolites are expressed as the mean ± SD concentration over Finger Mt. north $^{*}p < 0.05$, $^{**}p < 0.01$ against Finger Mt. south.

Biosynthesis starts from purine metabolism degradation (Hypoxanthine and Xanthine) and the intermediate Uric Acid. **Allallantoin pathway intermediates were stable and more abundant in the north exposure.** The amount of uric acid and allantoin decrease significantly in south samples ($p < 0.05$).

The allantoin plays an important protective role to excessive sun exposure; this pathway resulted over- expressed in the north exposed communities, where climatic conditions are more buffered and allow a successful settlement of endolithic colonization.

Allantoin is also produced in plants, providing protective function by blocking UV-B before it reaches cells, the consequences of UV-B exposure such as repairing damaged DNA.

The south exposed surface is in more prohibitive climatic conditions and in the shadow over the entire year, with limited possibility for metabolic activity and the need of a super-protective shield is of utmost importance for the survival of the community as a whole

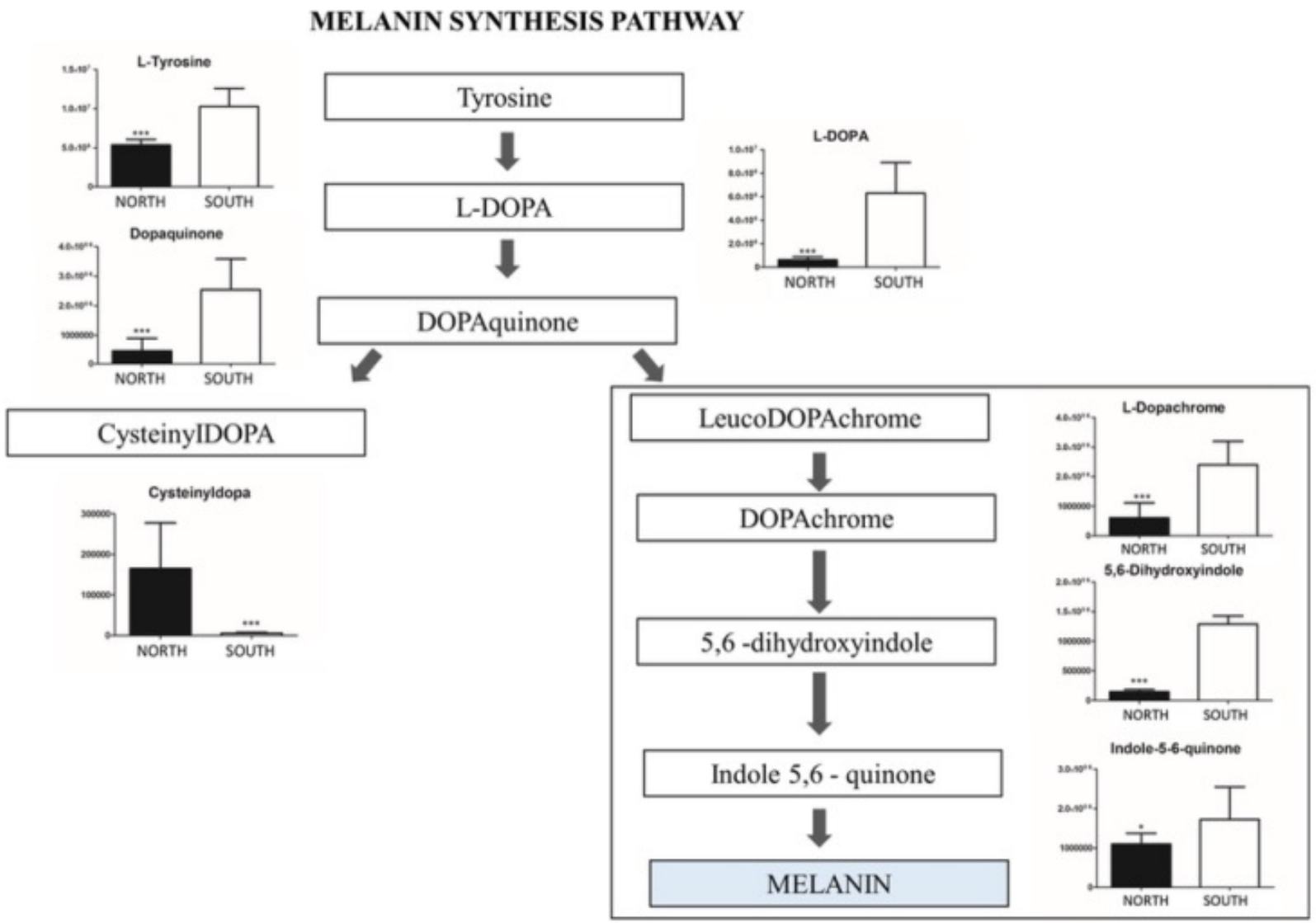

Fig 5. Melanin synthesis pathway. The conversion of tyrosine to melanin involves several steps and we found overall up-regulation of Finger Mt. south intermediates whereas Cysteinyl DOPA decreases, confirming that samples from south increase the synthesis of melanin. Metabolites are expressed as the mean ± SD concentration over Finger Mt. north $^{*}p < 0.05$, $^{**}p < 0.01$ against Finger Mt. south.

Melanin is produced starting from oxidation of amino acid L-Tyrosine.

We identify the tyrosine metabolism intermediates.

The pathway lead to the synthesis of melanin instead of cysteinyl DOPA.

All the intermediates (leucoDOPAchrome, DOPAchrome, 5–6 dihydroxy indole, Indole 5,6 quinone) reached the maximum level in south exposed samples ($p < 0.05$), **we have considered the melanin biosynthesis significantly enhanced in southern exposed rocks**.

Melanins **are ancient biological pigments found in all kingdoms of life and, in particular in the fungal kingdom, Melanin has been referred to as 'fungal armor'** due to the ability of **the polymer to protect microorganisms against a broad range of toxic insults.**

CONCLUSION

These results clearly indicate that opposite insolation selected organisms in the communities with different adaptation strategies in terms of key metabolites produced.

Metabolic response shifts across variations due to sun exposure, and giving insights on the capabilities of these ultimate ecosystems to sustain their growth and survival in such harsh environments.

We validated application of an untargeted metabolomics method that provides optimal identification of a wide range of metabolites to detect metabolic changes in the main pathways, determining which products are being released into the environment.

Urine Metabolome during Parturition

F. Gevi, A. Meloni, ...A. Ragusa, A.M. Timperio Metabolites 2020, *10*(7),290

Summary

UNIVERSITÀ DEGLI STUDI DELLA TUSCIA

DIPARTIMENTO DI SCIENZE ECOLOGICHE E BIOLOGICHE

1. **We analyzed metabolic changes during human childbirth labor.**
2. **We studied urine samples from 15 healthy pregnant women.**
3. **We collected samples before the onset of labor (out of labor, OL). and during labor (in labor or dilating phase, IL-DP).**
4. **We used (HILIC-UPLC-MS).**
5. **We performed multivariate statistical analysis grouped by metabolic pathway.**
6. **The differences belonged to steroid hormone: conjugated estrogens and amino acids much of this difference is determined by the fetal contribution.**

Metabolites. 2020 Jul; 10(7): 290. Urine Metabolome during Parturition

Urine Metabolome during Parturition

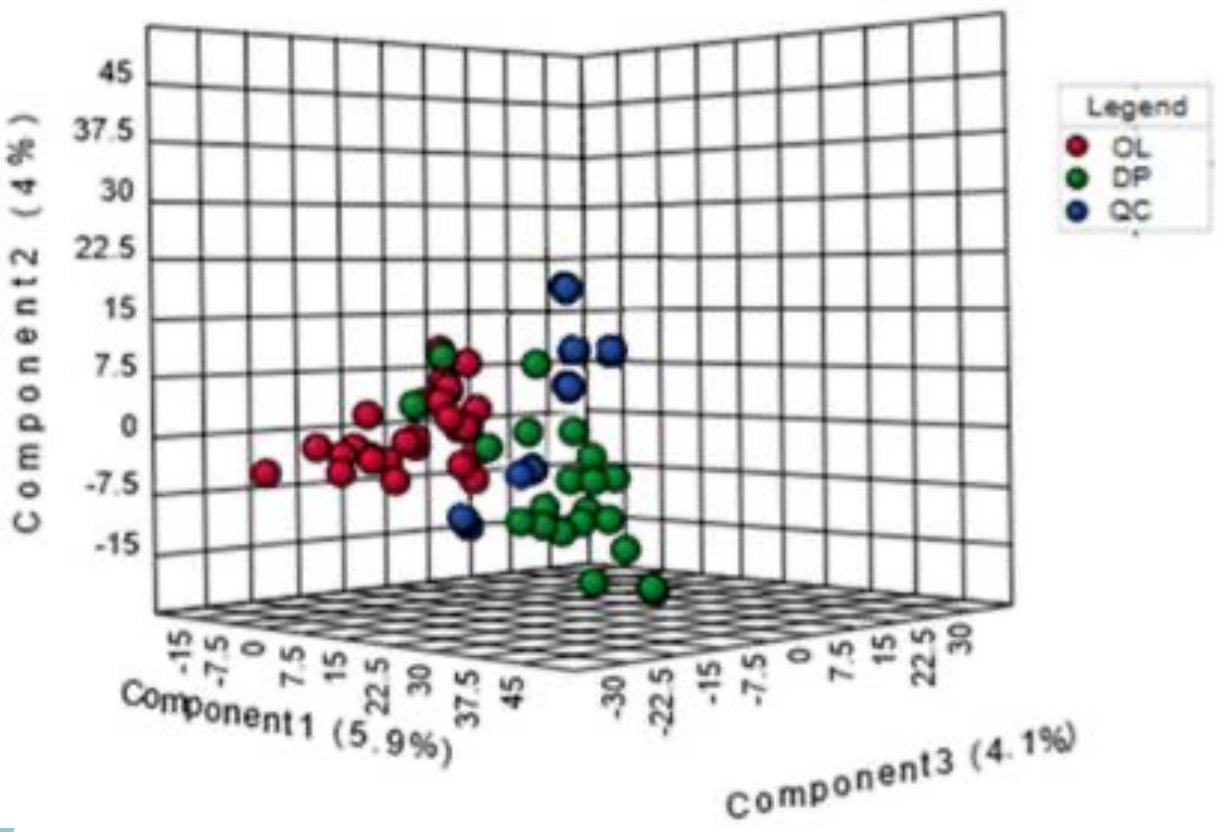

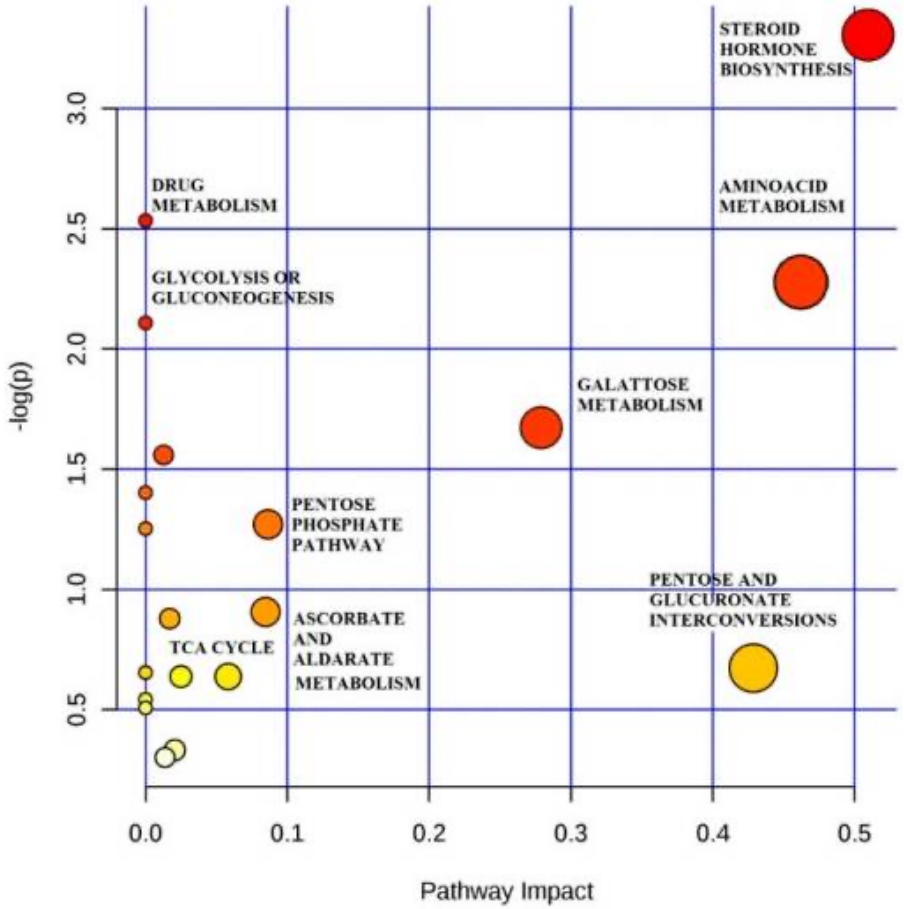

PLS-DA 3D plot based on normalized and mean-centered data. **Each data point represents the metabolome of a single individual. In red are expressed sample collected in OL. In green are expressed samples collected in IL-DP. In blue are expressed QC.**
Here you can see the statistical analysis PLS-DA the samples form clusters

We focalized our attention on this two metabolism Metabolic Pathway Analysis (MetPA) The color and size of each circle are based on the p-value and pathway impact value respectively.

Metabolites. 2020 Jul; 10(7): 290. Urine Metabolome during Parturition

Urine Metabolome during Parturition

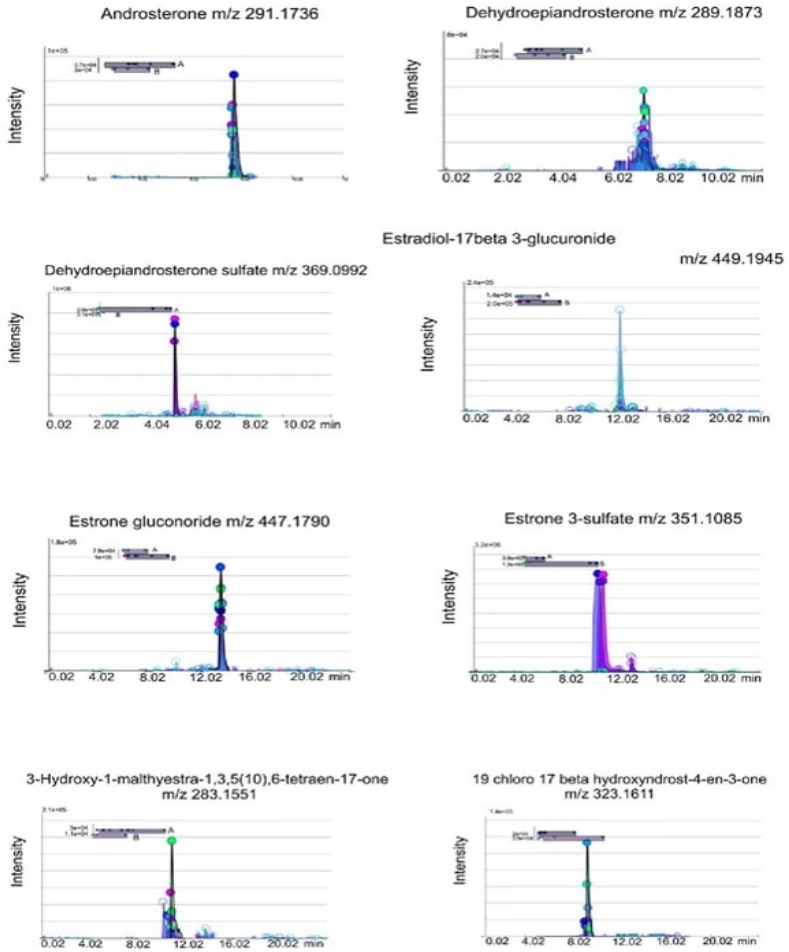

Estroni	Molecular weight	Detection mode	Out of labour (OL)	Dilating phase (DP)	Retention Time (RT) min	Percentual (%)
3 hydroxy2-methyl-1H-quinolin-one	175.05	Positive	9300	95000	7:00	3% ↑
19 chloro19-Chloro-3beta-hydroxyandrost-5-en-17-one = dehydroepiandrosterone	365.1695	Positive	20000	39000	5:0035	95% ↑
Androst-5-ene-3beta,17beta-diol= androsterone	290.1736	Positive	28000	22000	7:50	21% ↓
Androsterone	290.1736	Positive	28000	22000	7:50	21% ↓
Dehydroepiandrosterone Sulfate	369.0992	Positive	39000	3100	5:05	92% ↓
Dehydroepiandrosterone	288.1873	Positive	27000	26000	7:30	3% ↓
Pregnanediol	321.2145	Positive	8000	6000		25% ↓
3-Hydroxy-1-methylestra-1,3,5(10),6-tetraen-17-one	283.1551	Negative	30000	1000	5:50	63% ↑
Tetrahydrocortisone	365.1592-	Positive	140000	16000	6:30	88% ↓
Estrone 3 sulfate	351.1085	Positive	13800	130000	11:00	>100% ↑
Estrone gluconoride	447.1790	Positive	79000	10000	12:30	87% ↓
Estradiol 17 beta 3 gluconoride	449.1945	Positive	14000	20000	12:00	42% ↑

Electron ion chromatograms (EICs) of estrogens (A) Samples collected in OL and (B) collected in IL-DP. The circle at the top of each EIC, represents an auto-generated quality score, with larger circles denoting higher quality of extraction. Estrogen peaks were obtained with a 5 ppm window, representing the mass accuracy of the instrument.

Estrogen amount extracted from the urine in the two stages of pregnancy (OL and IL-DP). The excretion rate was calculated as the percentage ratio between the samples extracted in the two phases, considering for each of them as 100% of the total hormones found.

Urine Metabolome during Parturition

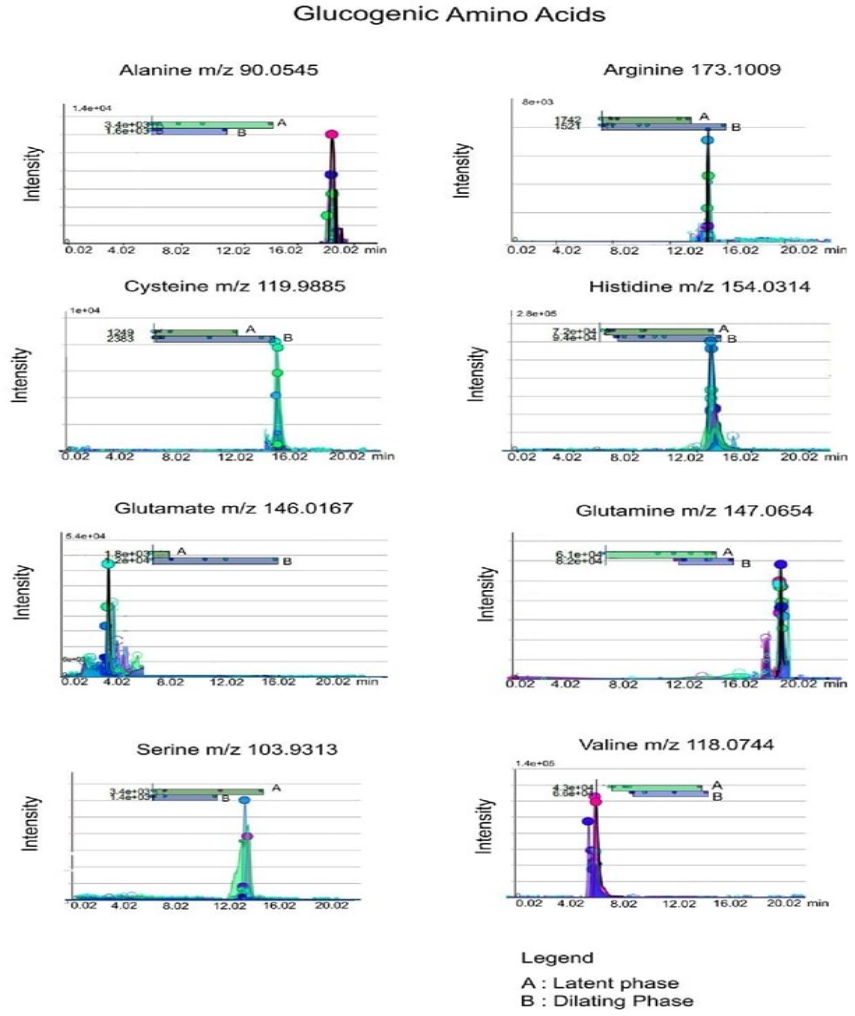

Glucogenic amico acid	Molecular weight	Detection mode	Out of labour (OL)	Dilating phase (DP)	Retention Time (RT) min	Percentual (%)
Ser	105.09	negative	3400	1400	12:02	59% ↓
Val	117.15	positive	43000	66000	6:00	35% ↑
His	155.15	negative	72000	94000	13:04	23% ↑
Arg	174.20	negative	1542	1742	14:00	11% ↑
Cys	121.16	negative	1249	2383	15:50	47% ↑
Ala	89.09	positive	3400	1600	20:02	47% ↓
Glu	147.13	negative	1800	12000	4:02	85% ↑
Gln	146.14	positive	61000	82000	21:00	25% ↑
Ketogenic amino acid	**Molecular weight**	**Detection mode**	**Out of labour (OL)**	**Dilating phase (DP)**	**Retention Time (RT) min**	**Percentual (%)**
Leu	131.17	positive	16000	26000	3:50	38% ↑
Lys	146.19	negative	3900	9700	19:00	60% ↑
Glucogenic and ketonic	**Molecular weight**	**Detection mode**	**Out of labour (OL)**	**Dilating phase (DP)**	**Retention Time (RT) min**	**Percentual (%)**
Ile	131.17	positive	16000	26000	12:00	38% ↑
Thr	119.12	positive	5600	6800	18:00	18% ↑
Phe	165.19	positive	180000	160000	17:00	11% ↓
Tyr	181.19	positive	170000	150000	5:00	12% ↓

Electron- ion chromatograms (EICs) of glucogenic amio acids (A) Samples collected in OL and (B) collected in DP. The circle at the top of each EIC, represents an auto-generated quality score, with larger circles denoting higher quality. Aminoacids peaks were obtained with a 5 ppm window, representing the mass accuracy of the instrument.

Aminoacids amount extracted from the urine in the two stages of pregnancy (OL and IL-DP). The excretion rate was calculated as the percentage ratio between the samples extracted in the two phases.

Urine Metabolome during Parturition

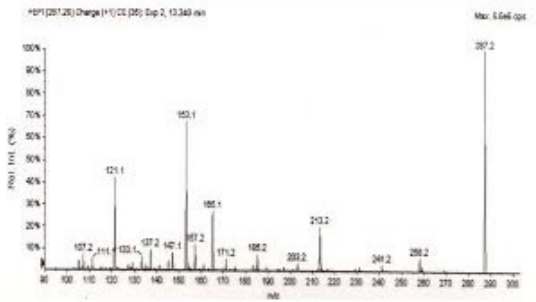

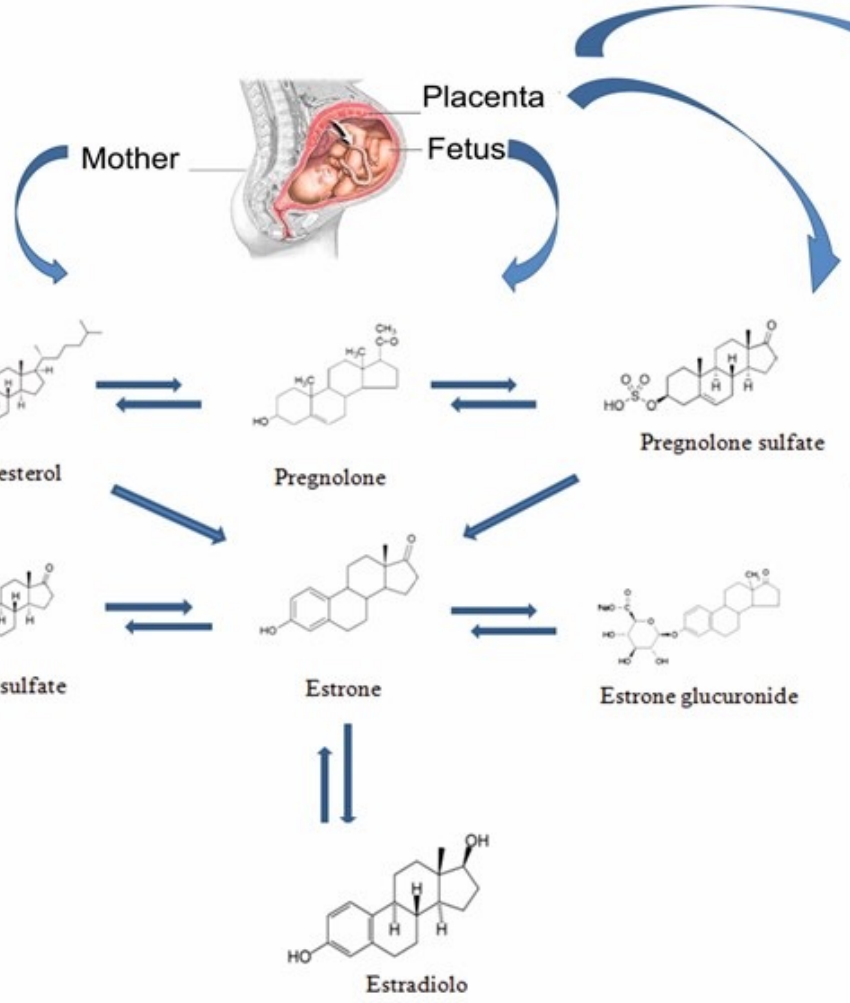

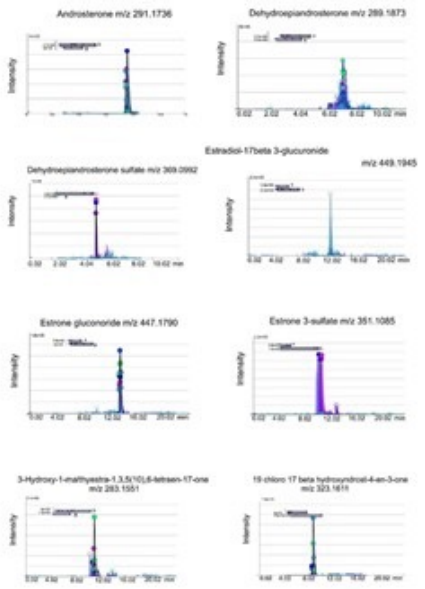

The increased excretion during labor of conjugated estrogens observed in our study may confirm the coordinated role played between the fetus and the mother during labor.

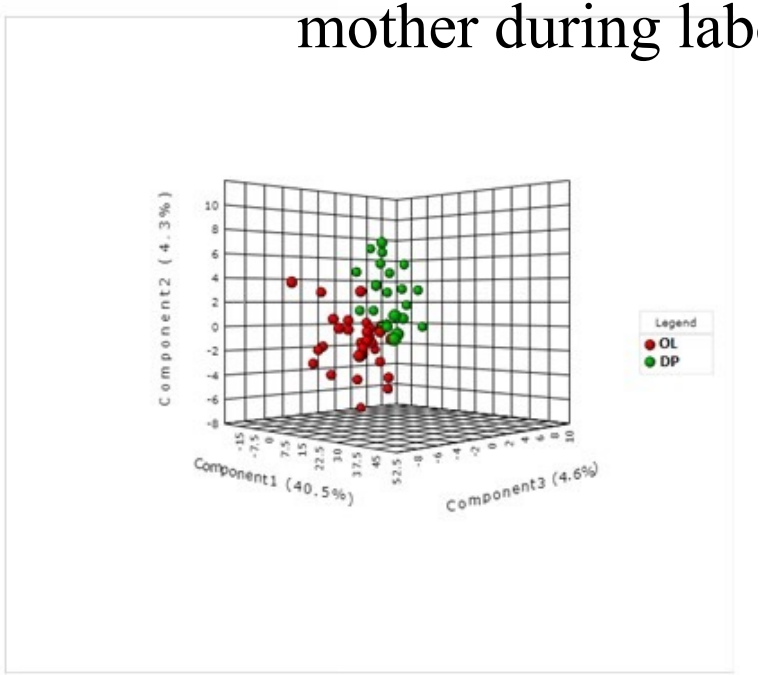

UNIVERSITÀ DEGLI STUDI DELLA TUSCIA
DIPARTIMENTO DI SCIENZE ECOLOGICHE E BIOLOGICHE

Plastic and Placenta: Identification of polyethylene glycol (PEG) compounds in the human placenta by HPLC-MS/MS system

the placenta samples come from the hospital

SAMPLE COLLECTION

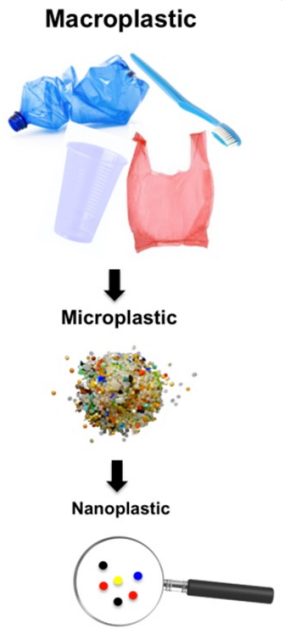

+

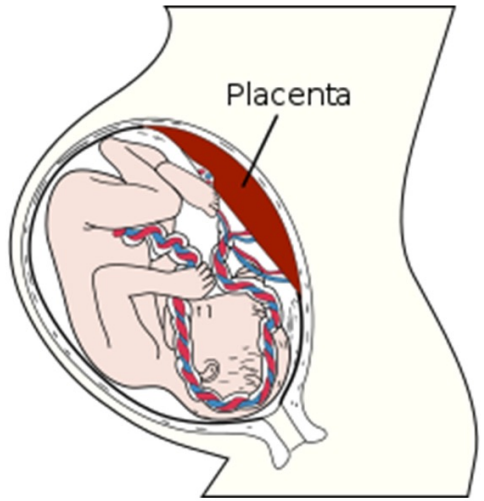

PLASTIC FREE METABOLIC EXTRACTION

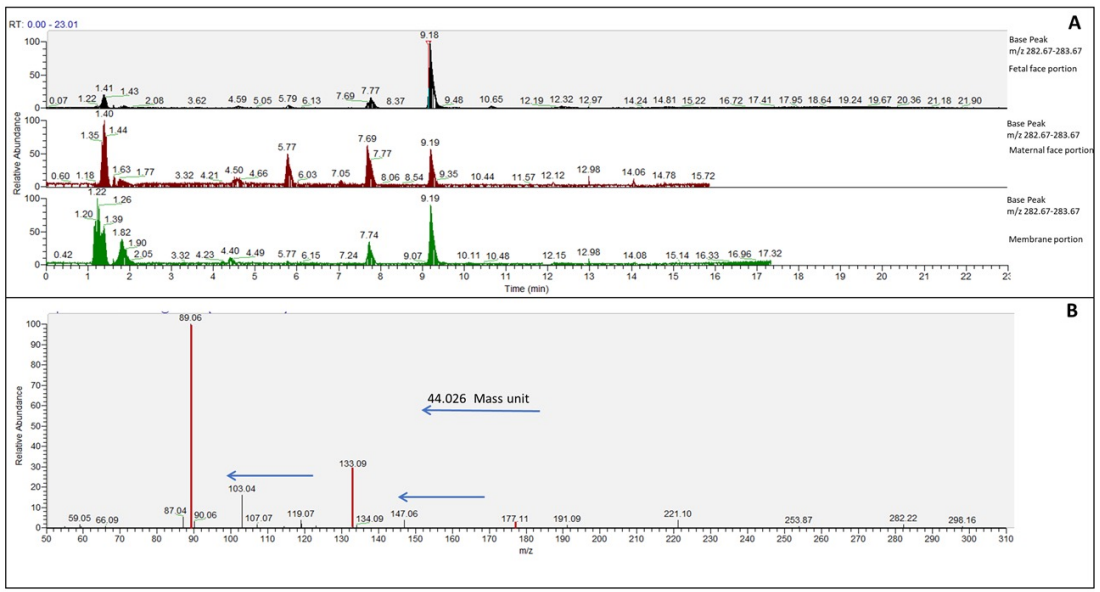

PEG - IDENTIFICATION

MASS SPECTROMETRY ANALYSIS

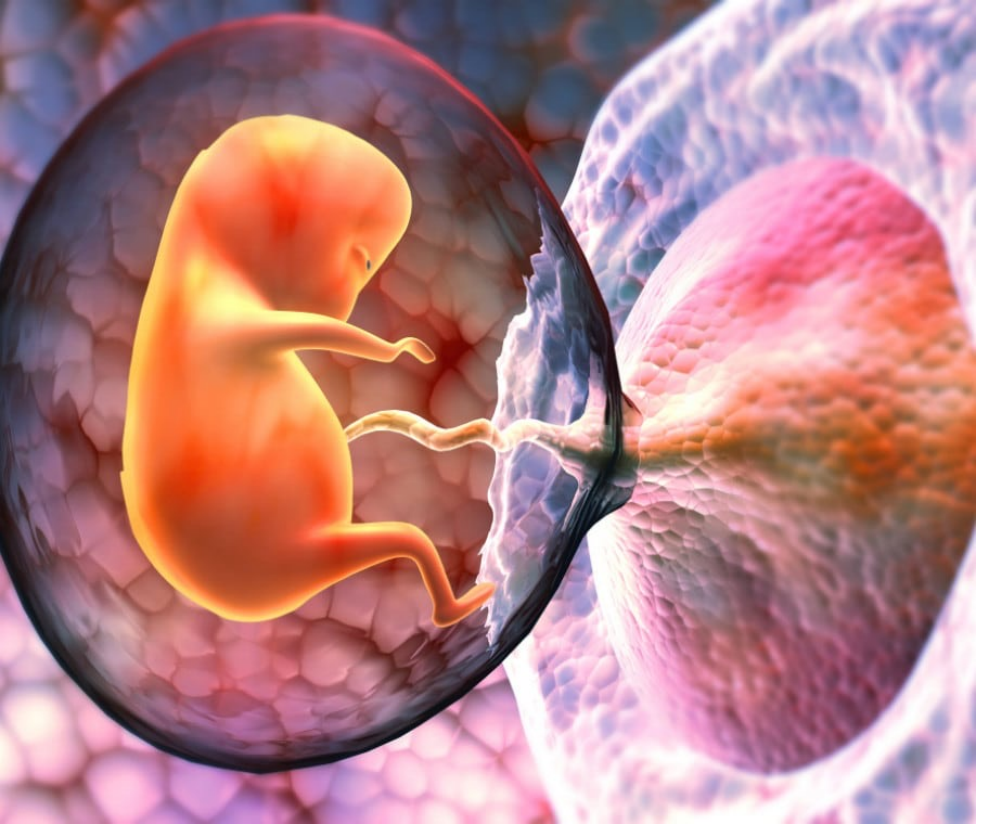

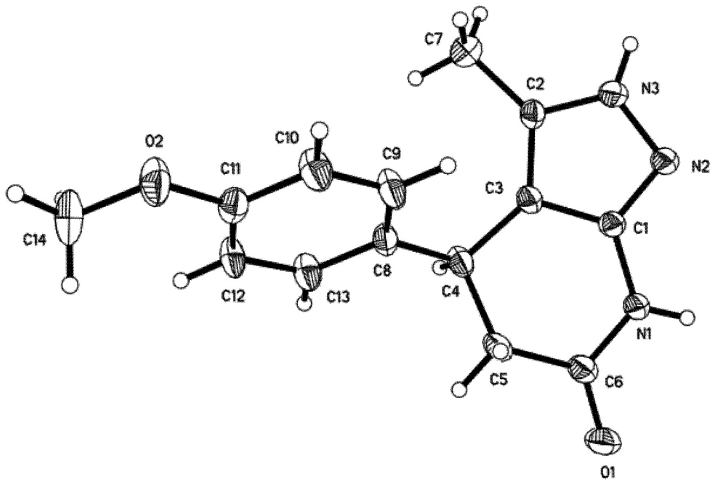

•We found the presence of PEG in ten of twelve placentas under examination.

Wide use of PEG in the preparation of medicines, foods, soaps, and personal care products.

•PEGs are frequently considered non-toxic to the human body however to assess the potential toxicity of this molecule.

•We focus on the potential toxicity of low molecular weight PEGs as they consist of fewer monomers (maximum 10).

•PEG is capable of spreading to any part of the examined placentas confirms that the PEG, once inside the human body, reaches the tissues of the placenta at all levels and is likely to find large concentrations.

•The absorption of PEG can depend on different physiological conditions and genetic characteristics, together with the diferent eating habits and lifestyles of the patients.

Identification of PEG polymers, 4 to 10 ethylene oxide monomers (EO-4 to EO-10) by HPLCS-MS / MS.

UNIVERSITÀ DEGLI STUDI DELLA TUSCIA
DIPARTIMENTO DI SCIENZE ECOLOGICHE E BIOLOGICHE

MEASURED MASS	PUTATIVE FORMULA	PUTATIVE IDENTIFICATION	CALCULATED EXACT MASS
195.1228	$C_8H_{18}O_5$	PEG-EO4	195.1227
239.1489	$C_{10}H_{22}O_6$	PEG-EO5	239.1489
283.1752	$C_{12}H_{26}O_7$	PEG-EO6	283.1751
327.2018	$C_{14}H_{30}O_8$	PEG-EO7	327.2013
371.2284	$C_{16}H_{34}O_9$	PEG-EO8	371.2276
415.2542	$C_{18}H_{38}O_{10}$	PEG-EO9	415.2538
459.2801	$C_{20}H_{42}O_{11}$	PEG-EO10	459.2800

UNIVERSITÀ DEGLI STUDI DELLA TUSCIA
DIPARTIMENTO DI SCIENZE ECOLOGICHE E BIOLOGICHE

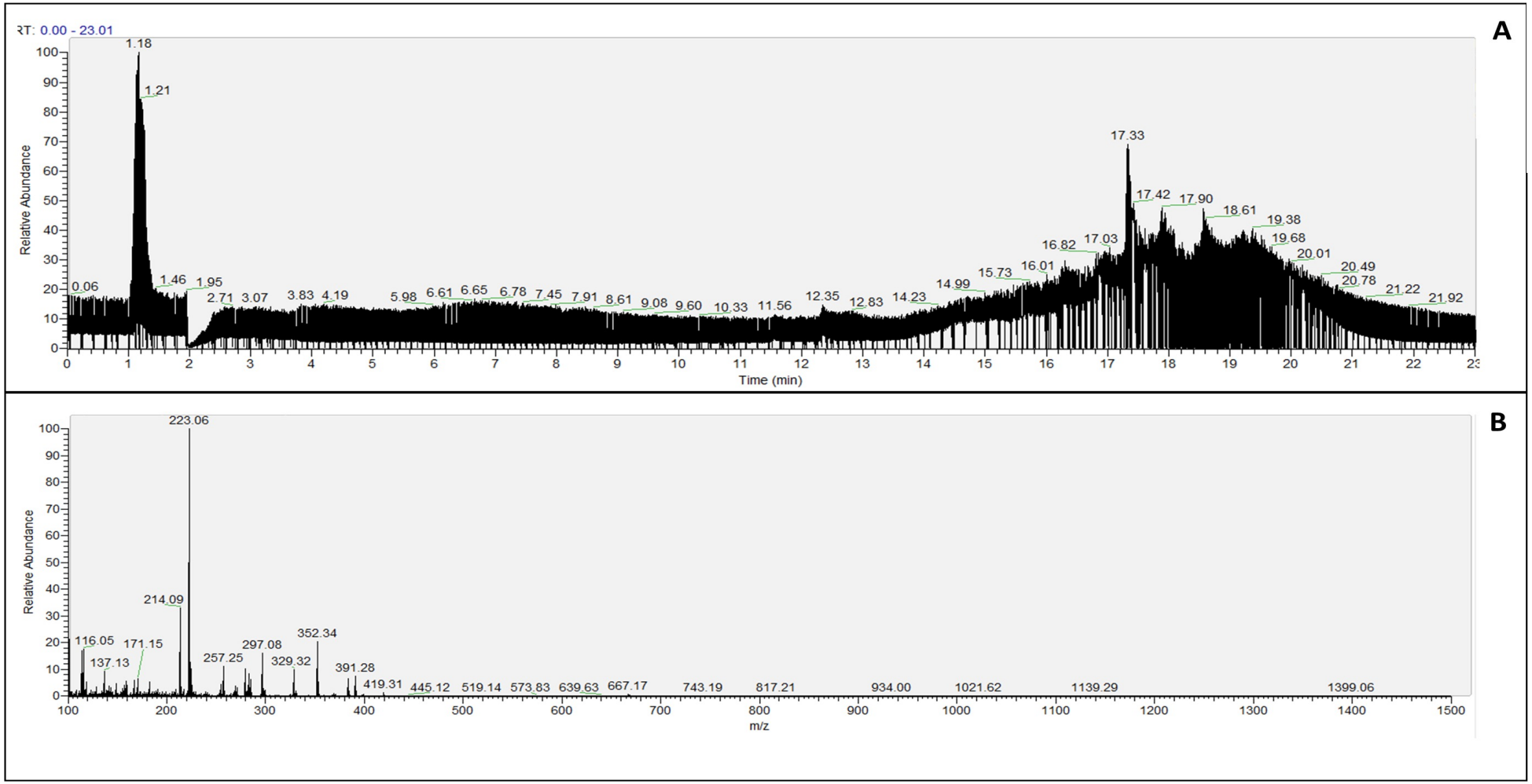

Panel A represents the TIC of the analytical blank considered control sample.
Panel B represents the spectrum in MS / MS of the analytical blank.

Data collection and processing was performed by using software packages within the system as described in the materials and methods section. For each portion of samples several masses have been annotated. These masses were related to an ethylene oxidative from 4 monomers to 10 (EO-4 to EO-10) of PEGs as shown in Table 1.

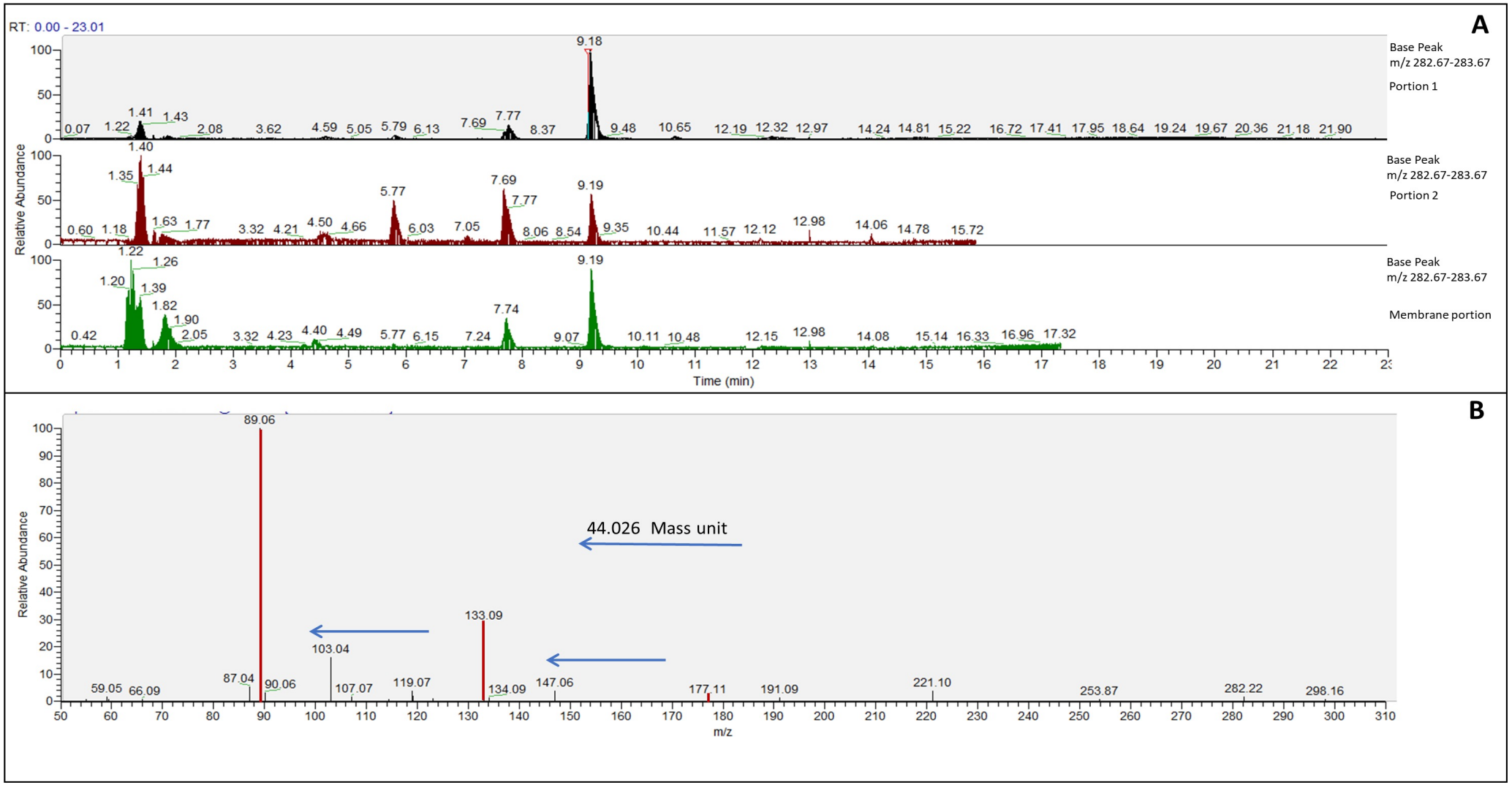

Panel A: Base peak chromatogram of 283.17 m/z of all portions collected from sample #6.
Panel B: A MS/MS spectrum showing the differences in mass of the polypropylene glycol series (44.0262 mass units). for each placenta we took three different samples in three different areas

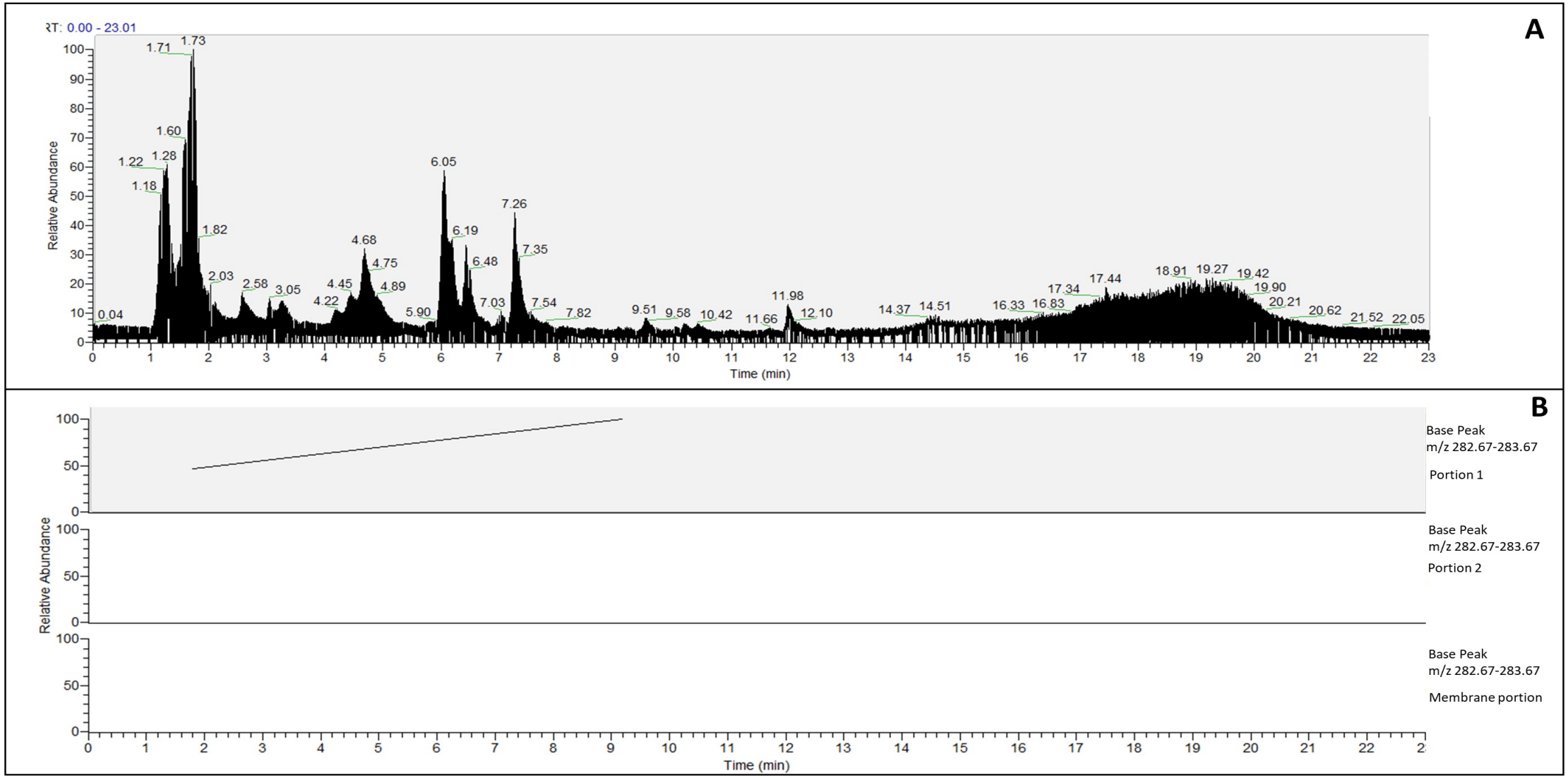

Panel A: The spectrum showing the absence of 283.17 m/z in Placenta #4bis considered control samples.

Panel B: Base peak chromatogram of 283.17 m/z of three portions were collected from sample Placenta #4bis.

Putative Formula	Putative Identification	Calculated Exact Mass		1bis	2bis	3	3bis	4	4bis	5	6	7	8	9	10
$C_{12}H_{26}O_7$	PEG-EO6	283.1752	Portion 1	*	*	*	*	*	-	*	*	*	*	*	-
			Portion 2	*	*	*	*	*	-	-	*	*	*	*	-
$C_{14}H_{30}O_8$	PEG-EO7	327.2013	Portion 1	*	*	-	*	-	-	*	*	*	-	-	-
			Portion 2	*	*	*	*	*	-	*	*	*	*	*	-
$C_{16}H_{34}O_9$	PEG-EO8	371.2276	Portion 1	*	*	*	*	-	-	*	*	*	*	-	-
			Portion 2	*	*	*	-	*	-	*	*	-	*	*	-
$C_{18}H_{38}O_{10}$	PEG-EO9	415.2538	Portion 1	-	*	-	-	-	-	*	*	-	*	-	-
			Portion 2	-	*	-	*	*	-	*	-	*	*	*	-
$C_{20}H_{42}O_{11}$	PEG-EO10	459.2800	Portion 1	-	*	-	-	-	-	*	-	*	-	-	-
			Portion 2	-	-	-	*	-	-	*	-	*	*	*	-

Table 2a. Placenta Portion.

The symbol "*" represents the presence of the PEG fragment in the sample.

Putative Formula	Putative Identification	Calculated Exact Mass	1bis	2bis	3	3bis	4	4bis	5	6	7	8	9	10
$C_{12}H_{26}O_7$	PEG-EO6	283.1752	*	*	*	*	*	-	*	*	*	*	-	-
$C_{14}H_{30}O_8$	PEG-EO7	327.2013	-	*	-	*	*	-	*	-	-	-	-	-
$C_{16}H_{34}O_9$	PEG-EO8	371.2276	-	*	-	*	*	-	*	*	*	-	-	-
$C_{18}H_{38}O_{10}$	PEG-EO9	415.2538	-	-	-	-	*	-	*	-	-	-	*	-
$C_{20}H_{42}O_{11}$	PEG-EO10	459.2800	-	-	-	-	-	-	*	*	-	-	*	-

Table 2b. Chorioamniotic Membrane Portion.
The symbol "*" represents the presence of the PEG fragment in the sample.

CONCLUSION

UNIVERSITÀ DEGLI STUDI DELLA TUSCIA
DIPARTIMENTO DI SCIENZE ECOLOGICHE E BIOLOGICHE

- slow clearance of large PEGs potential adverse effects
- accumulation in tissus particularly in the central nervous system.
- the presence of plastic in its various forms (PEG and microplastics) in the placenta, can alter the communication between fetal and maternal cells which in turn could occur during pregnancy.
- PEG can exert an immunological effect on human cells.

MASS SPECTROMETRY LAB

UNIVERSITÀ DEGLI STUDI DELLA TUSCIA

DIPARTIMENTO DI SCIENZE ECOLOGICHE E BIOLOGICHE

MASS SPECTROMETRY LAB

UNIVERSITÀ DEGLI STUDI DELLA TUSCIA
DIPARTIMENTO DI SCIENZE ECOLOGICHE E BIOLOGICHE

MALDI TOF-TOF

GC

micrOTOF-Q

UNIVERSITÀ DEGLI STUDI DELLA TUSCIA

DIPARTIMENTO DI SCIENZE ECOLOGICHE E BIOLOGICHE

SARA RINALDUCCI
FEDERICA GEVI
VERONICA LELLI
GIUSEPPINA FANELLI

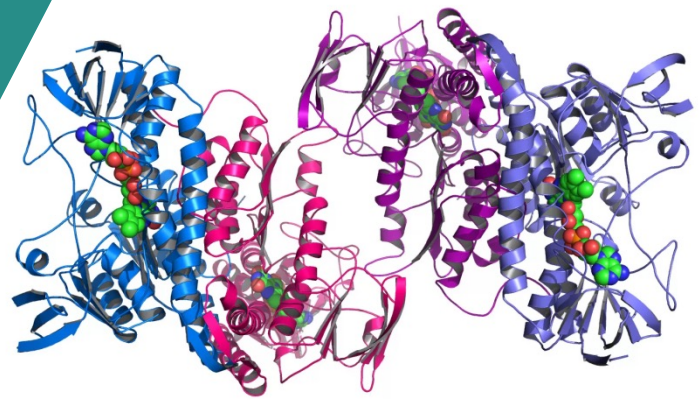

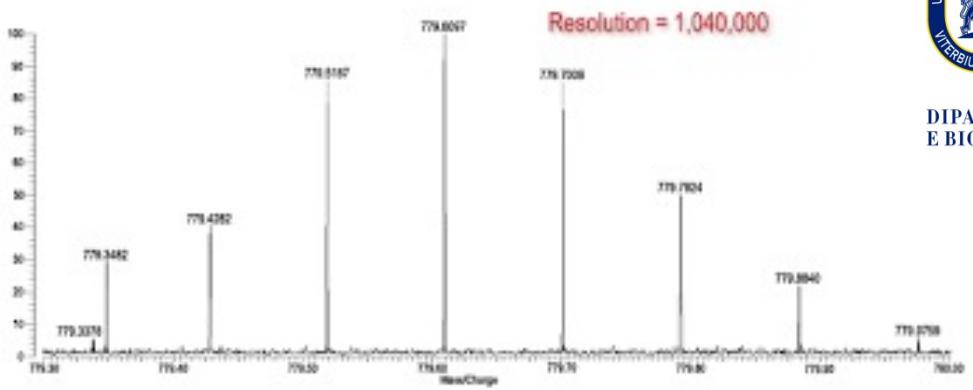

UNIVERSITÀ DEGLI STUDI DELLA TUSCIA

DIPARTIMENTO DI SCIENZE ECOLOGICHE E BIOLOGICHE

Thank you for your attention

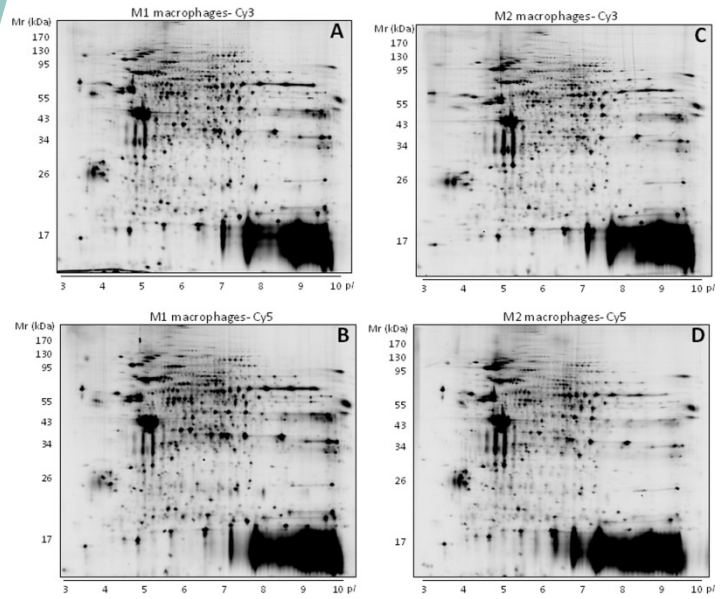

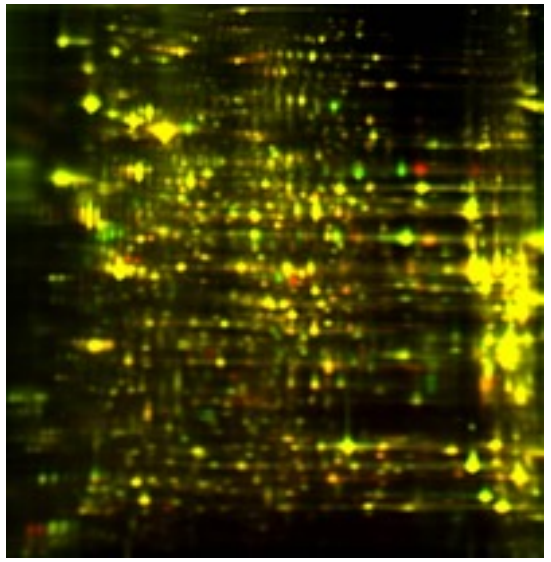

Metabolomics of Dry Versus Reanimated Antarctic Lichen-Dominated Endolithic Communities

Fanelli, G., Coleine, C., Gevi, F., ...Selbmann, L., Timperio, A.M. ***Life***, 2021, 11(2), pp. 1–13, 96

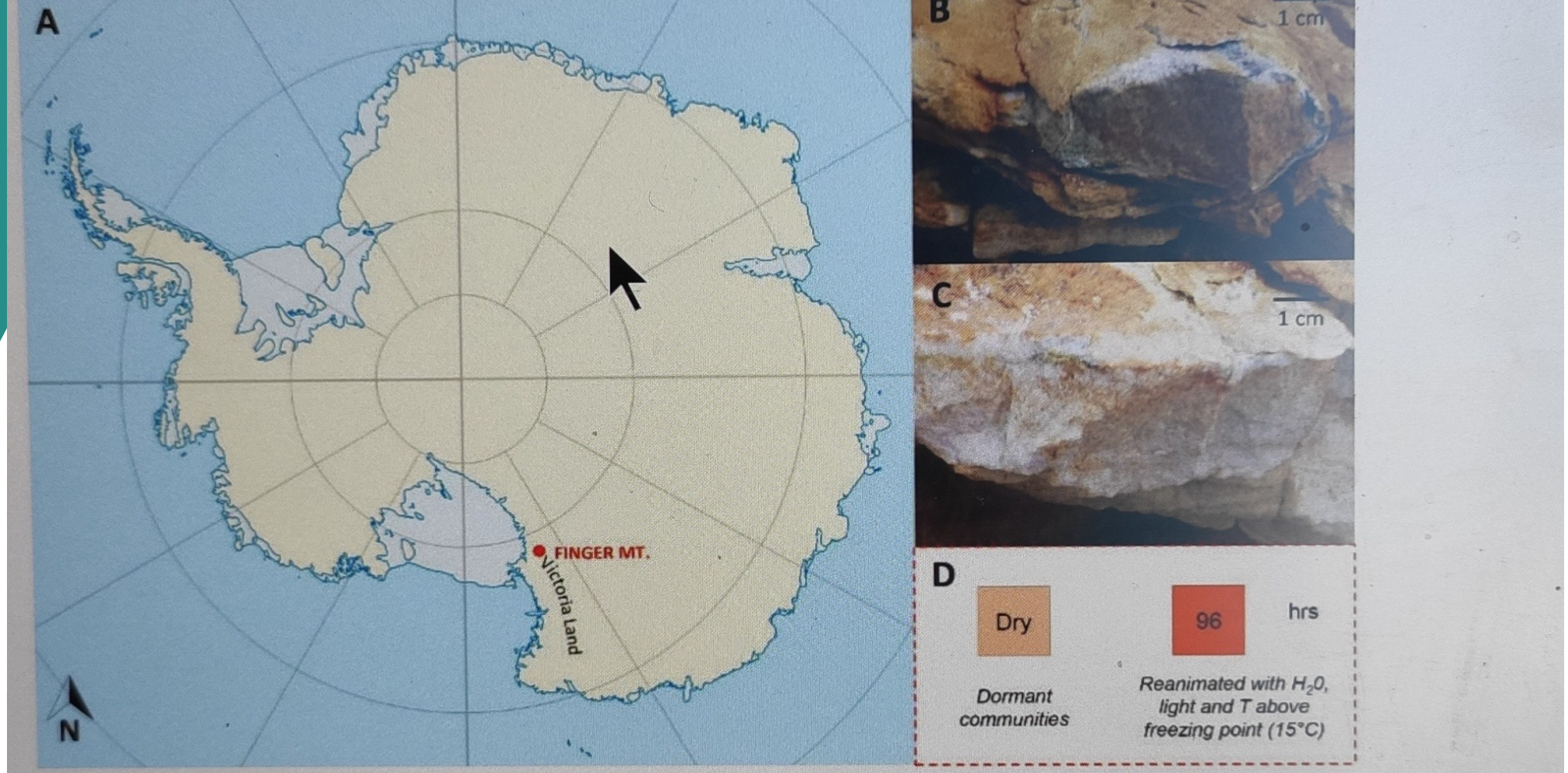

Figure 1. (**A**) Map of Antarctica. Red symbol indicates the study area, Finger Mt. (McMurdo Dry Valleys, Southern Victoria Land, Continental Antarctica); (**B**) Northern and (**C**) southern exposed rock surfaces; (**D**) outline of reactivation experiment. Credit by Italian National Antarctic Research Program (PNRA).

MAIN PURPOSE

compare the responses of Antarctic endolithic communities, both under dry conditions (i.e., when dormant), and after reanimation by wetting, light, and optimal temperature (15 °C).

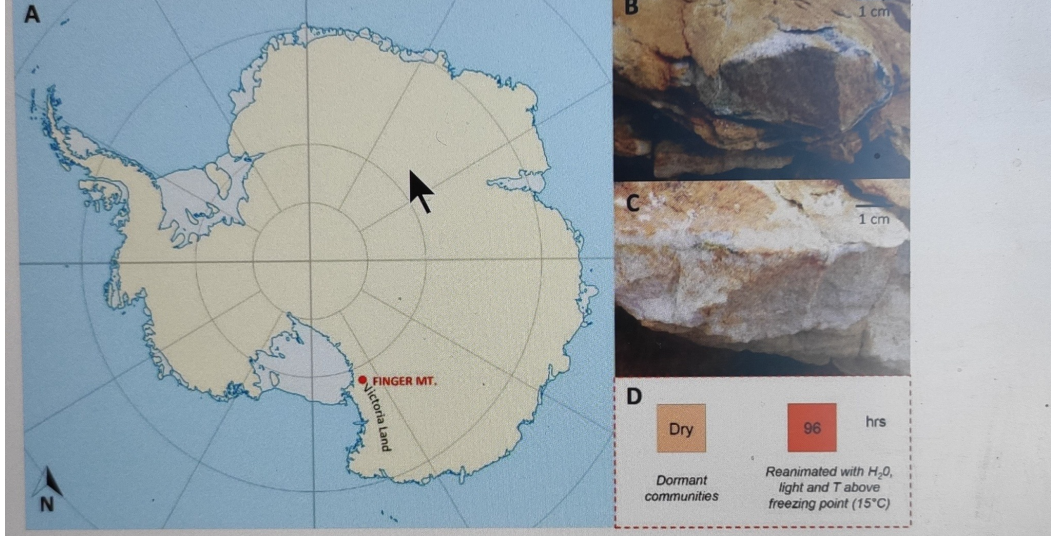

Figure 1. (**A**) Map of Antarctica. Red symbol indicates the study area, Finger Mt. (McMurdo Dry Valleys, Southern Victoria Land, Continental Antarctica); (**B**) Northern and (**C**) southern exposed rock surfaces; (**D**) outline of reactivation experiment. Credit by Italian National Antarctic Research Program (PNRA).

RESULTS

We found that several metabolites were differently expressed in reanimated opposite sun exposed communities:

- **the saccharopine pathway was up-regulated in the north surface**.
- the spermine/spermidine pathway was significantly down-regulated in the shaded exposed communities.
- **the carnitine-dependent pathway is up-regulated in south-exposed reanimated samples, indicating the preferential involvement of the B-oxidation for the functioning of TCA cycle**.

Workflow

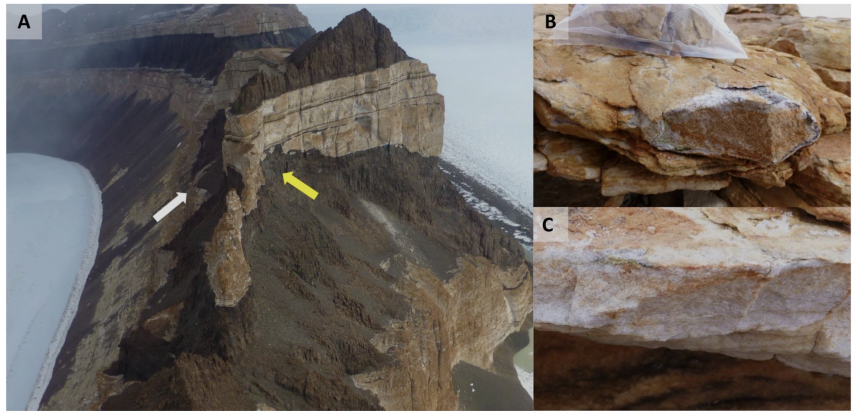

Fig 1. A) Finger Mt. landscape: the yellow arrow indicates the north exposed surface, while the white arrow indicates the south exposed surface; B) north exposed sandstone rock; C) south exposed sandstone rock.

Different Community Response North Dry Samples vs. North Reanimated Samples

Different Community Response South Dry Samples vs. South Reanimated Samples

Different Community Response North Reanimated Samples vs. South Reanimated Samples

HPLC-MS

the saccharopine pathway was up-regulated in the north surface.

the carnitine-dependent pathway is up-regulated in south-exposed reanimated samples, indicating the preferential involvement of the B-oxidation for the functioning of TCA cycle.

the spermine/spermidine pathway was significantly down-regulated in the shaded exposed communities

A

Different Community Response North Dry Samples vs. North Reanimated Samples

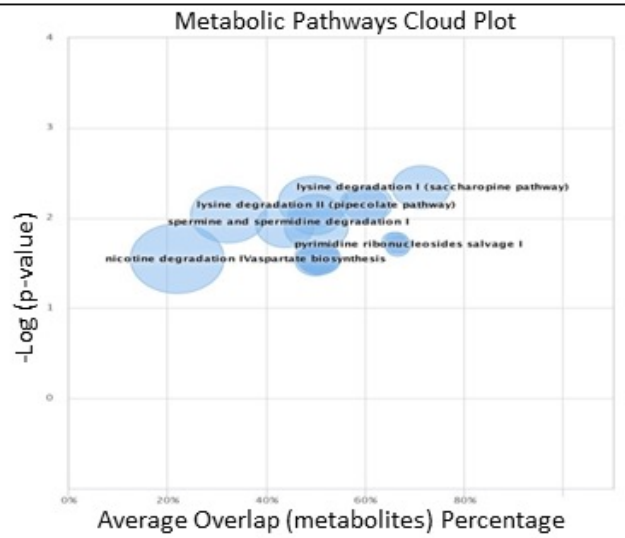

Pathways with a higher percent overlap of metabolites and statistical significance will appear in the upper right corner

We identified metabolites which were statistically significantly up- or down-regulated in reactivated northern exposed rocks

pathway **were up regulated** after metabolic machinery reactivation.

saccharopine and polyamines biosynthesis pathways that are tightly correlated with the growth, development, or reproduction of the organisms and energy metabolism and may play an important role when the communities face environmental changes in its living habitat.

B

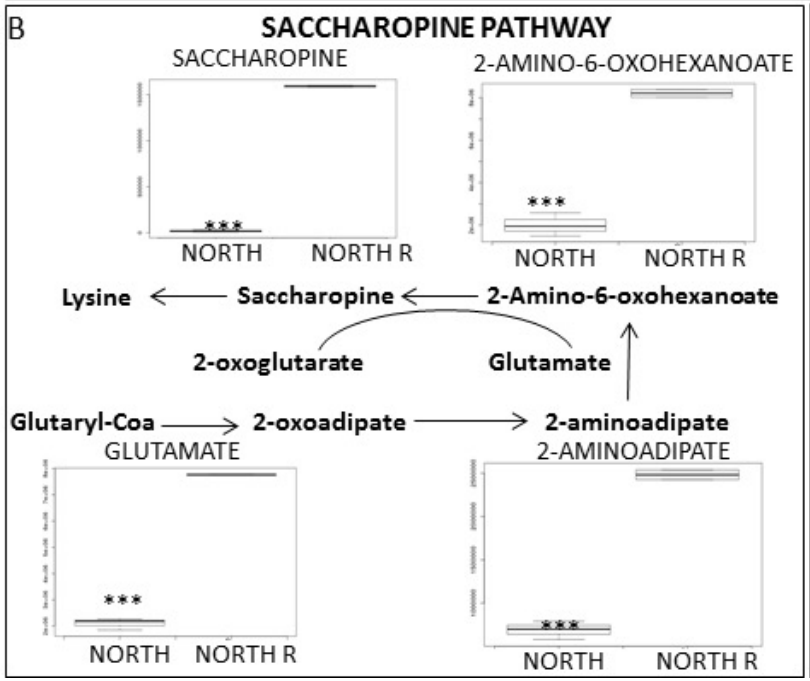

C

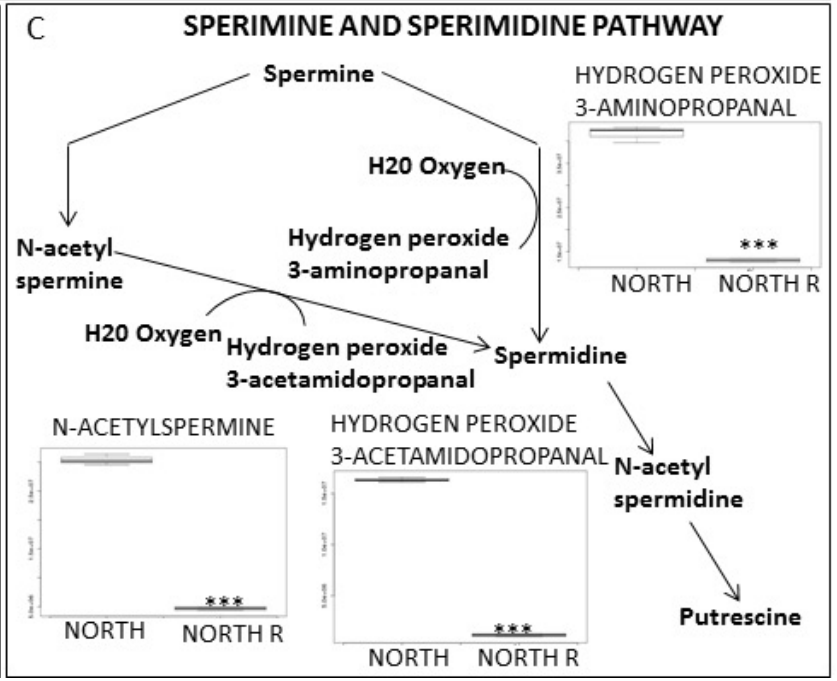

Each pathway is displayed as a circle, with the *x* axis representing the percentage of metabolite overlap within that pathway and the *y* axis representing increased pathway significance calculated from the pathway analysis.

A

Different Community Response South Dry Samples vs. South Reanimated Samples

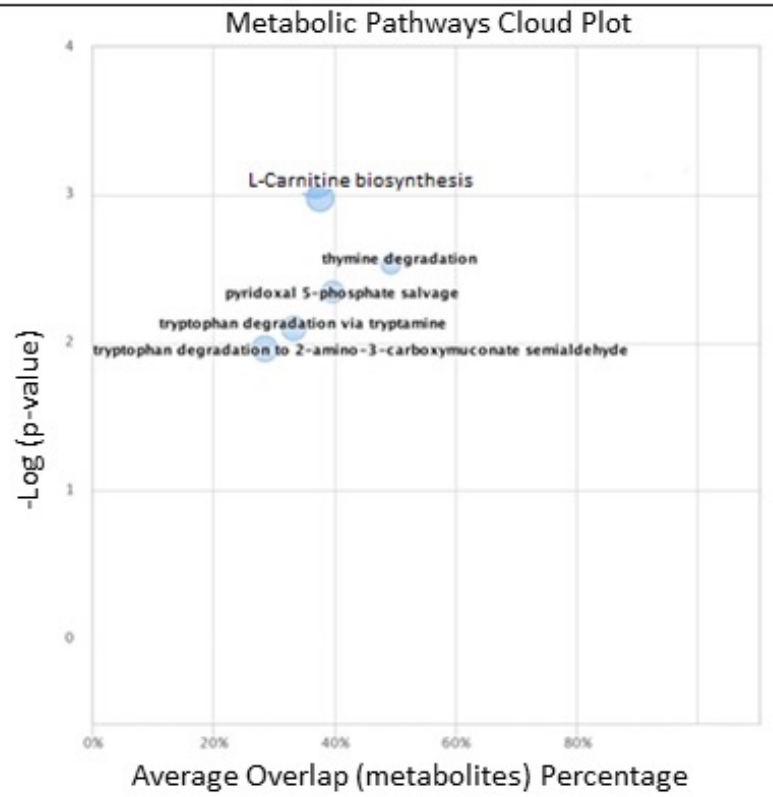

The most significant pathway **up-regulated** in reanimated south exposed samples is related to **carnitine biosynthesis.**

B

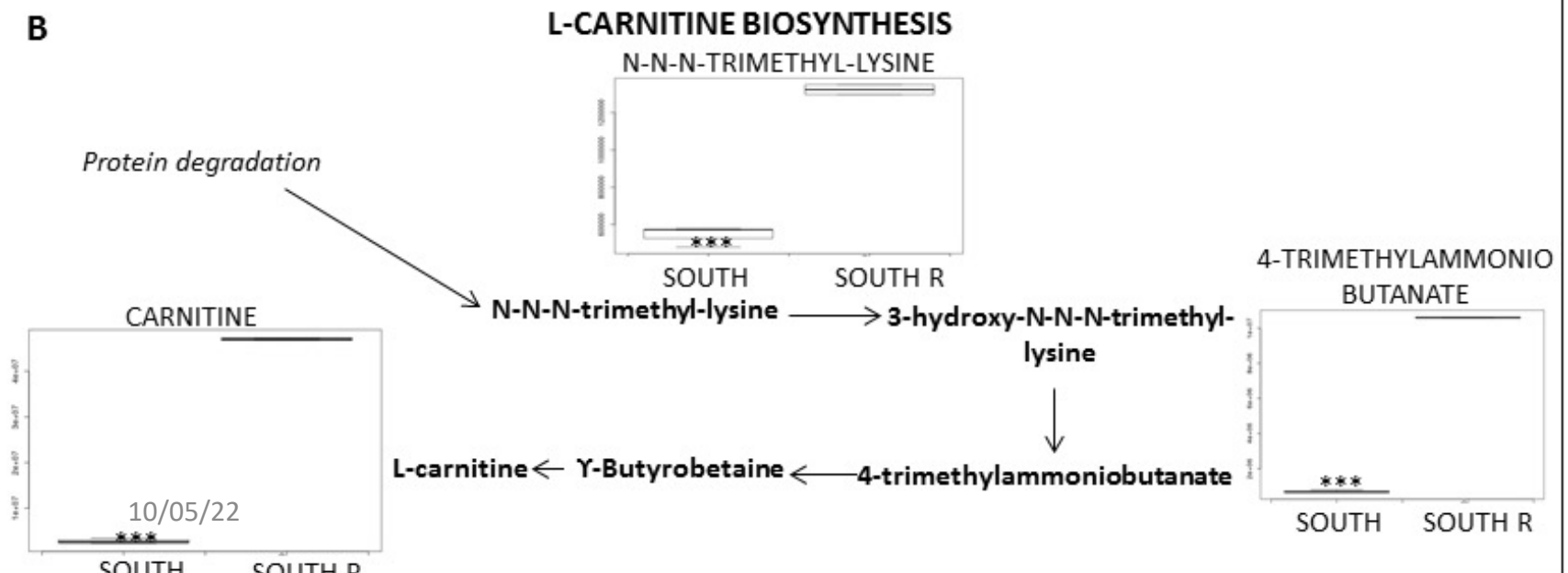

L-carnitine is synthesized from the essential amino acid lysine via a specific biosynthetic pathway; lysine is methylated to form ε-N-trimethyllysine in a reaction catalyzed by specific lysine methyltransferases that use S-adenosyl-methionine (derived from methionine) as a methyl donor. Then, ε-N-Trimethyllysine is released for carnitine synthesis by protein hydrolysis.

Different Community Response North Reanimated Samples vs. South Reanimated Samples

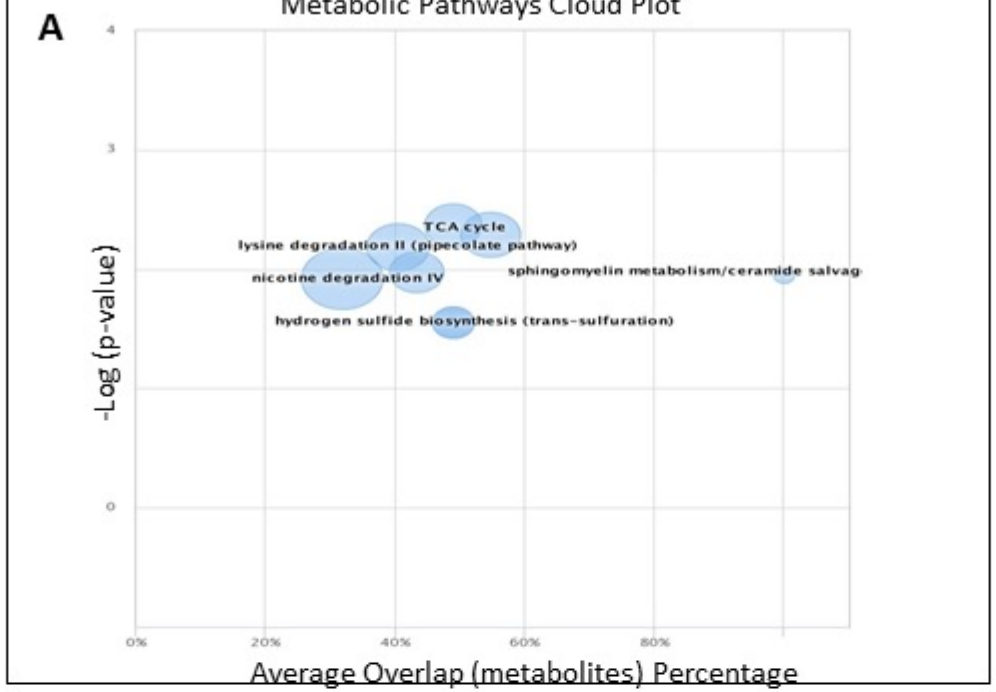

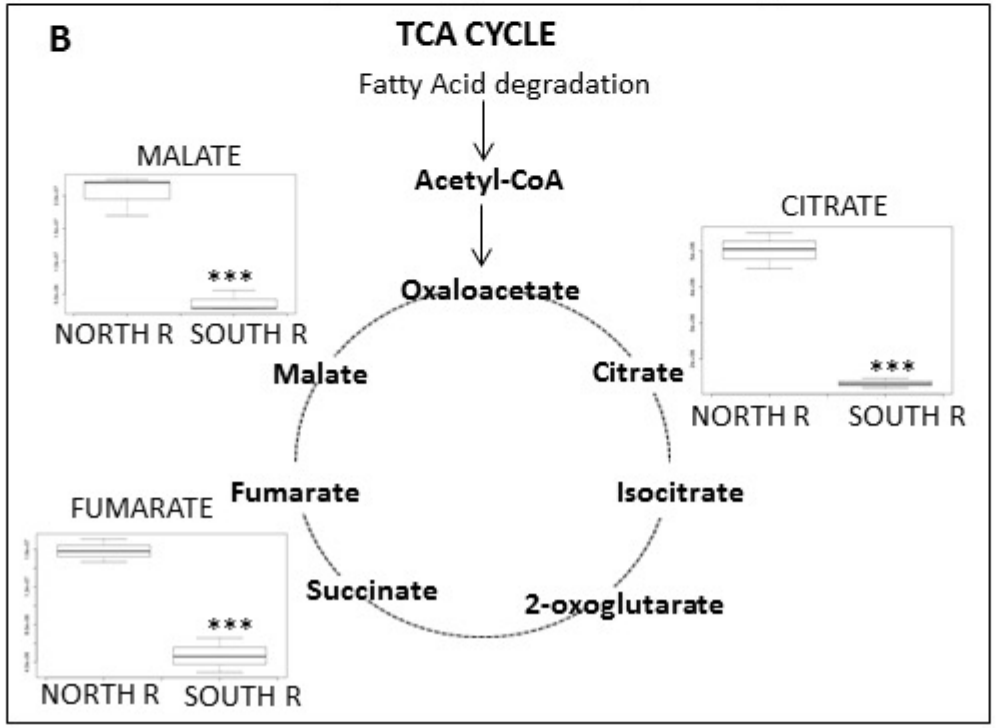

We also investigated differences/similarities in responses between northern and southern reanimated rock samples.
that the most influenced is the tricarboxylic acids (TCA) pathway.
In particular, we found that the **southern reactivated samples prefer the TCA pathway to restore their function**. An oxidation of the metabolic intermediates related to the TCA such as citrate, fumarate, and malate is shown .

Conclusions

Cryptoendolithic microbial ecosystems a model system for studies of microbial ecology in both hot and cold deserts.

Endolithic microorganisms exist in dormant states but rapidly reactivate the saccharopine and polyamines biosynthesis pathways that are tightly correlated with the growth, development, or reproduction of the organisms and energy metabolism and may play an important role when the communities face environmental changes in its living habitat.

we provided critical insights on how Antarctic endolithic communities respond to stresses, maintaining biological activities under harshest conditions that are typically incompatible with active life.

these findings will be useful in modelling predicting important pathways that have evolved to support these life-forms on the extreme edge of Antarctic desert.

These results may be also applied to microbial endolithic ecosystems in drylands worldwide, in an era of climate change and rapid desertification.

Detection and Comparison of Bioactive Compounds in Different Extracts of Two Hazelnut Skin Varieties, Tonda Gentile Romana and Tonda Di Giffoni, Using a Metabolomics Approach.

Metabolites 2021, 11, 296. https://doi.org/10.3390/metabo11050296

Detection and Comparison of Bioactive Compounds in Different Extracts of Two Hazelnut Skin Varieties, Tonda Gentile Romana and Tonda Di Giffoni, Using a Metabolomics Approach.

1. **Agro-wastes are one of the major sources for nutritional and therapeutic benefits along with other beneficial properties.**
2. **Dark brown pellicular pericarp (skin or testa), covering the hazelnut seed, is removed before consumption after the roasting of a kernel.**
3. **hazelnut varieties, Tonda Gentile Romana and Tonda di Giffoni, were profiled by a metabolomics-based approach.**
4. **significant qualitative and quantitative metabolic differences were observed between them.**
5. **Samples were also assessed for their total phenolic and antioxidant capacity using two different assays.**
6. **These results indicated that hazelnut skin, especially from the Romana variety, could potentially be used as an ingredient in healthy food.**

Metabolites 2021, 11, 296. https://doi.org/10.3390/metabo11050296

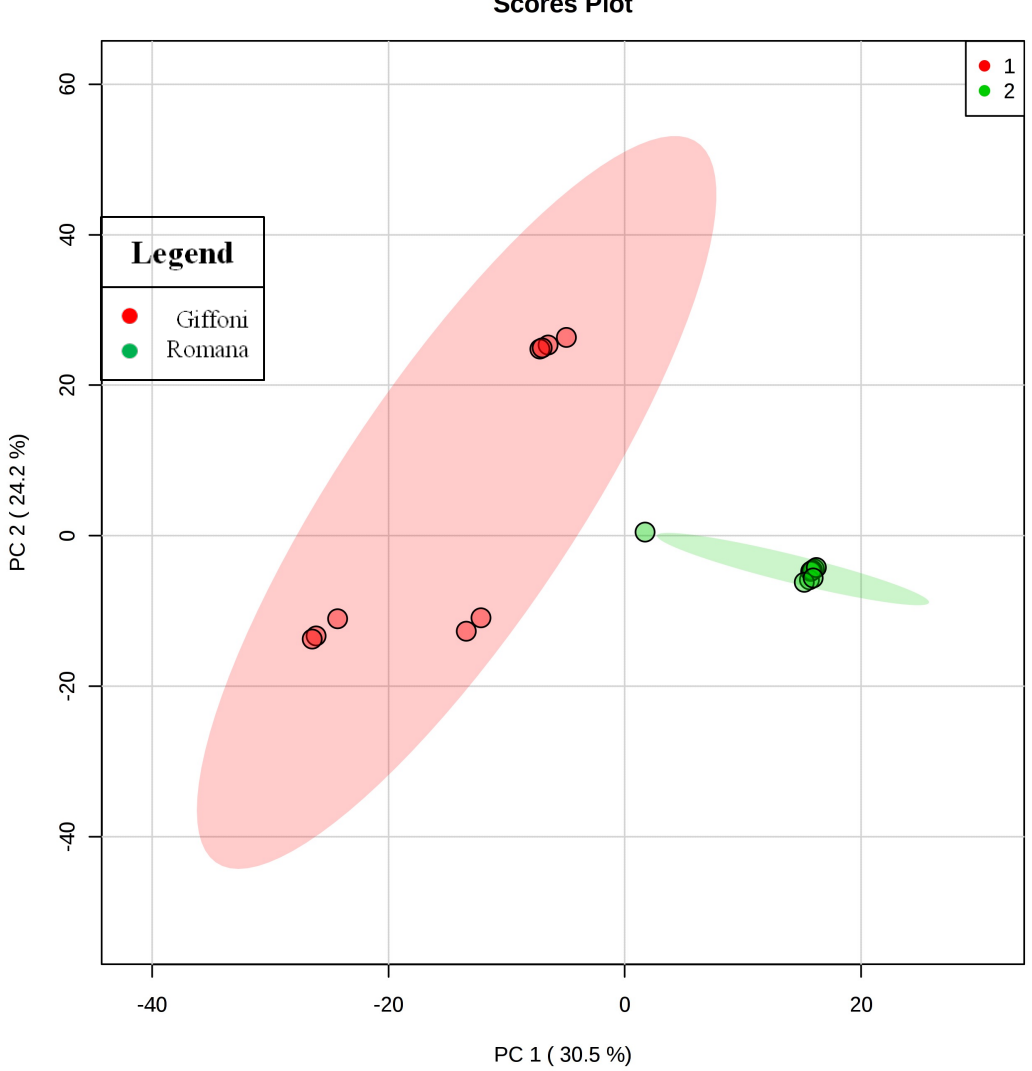

Figure 1. Principal component analysis (PCA) scores plot . The PCA scores plot shows a clear segregation of Giffoni and Romana samples, indicating that Giffoni and Romana have different metabolic profiles.

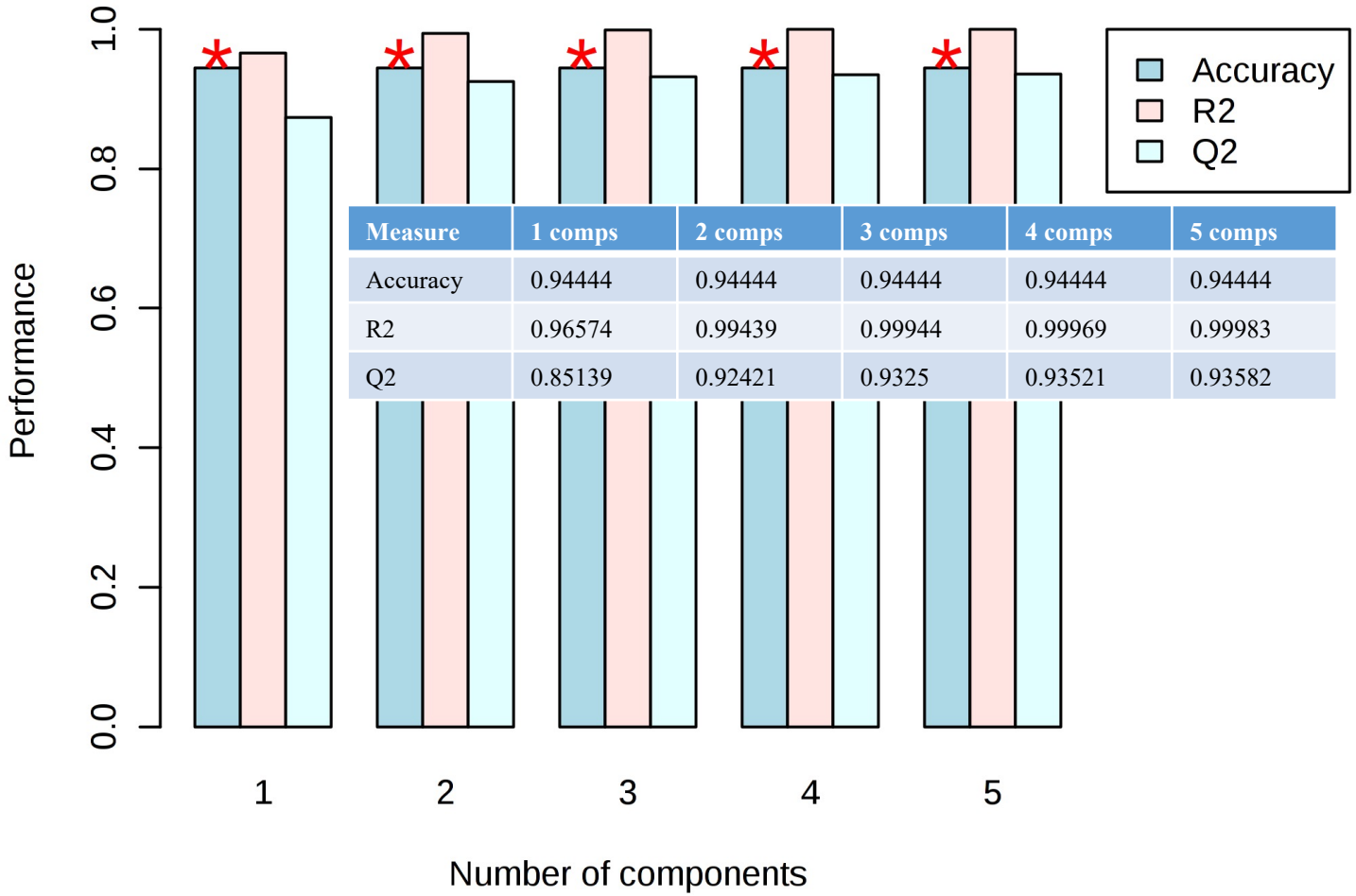

Measure	1 comps	2 comps	3 comps	4 comps	5 comps
Accuracy	0.94444	0.94444	0.94444	0.94444	0.94444
R2	0.96574	0.99439	0.99944	0.99969	0.99983
Q2	0.85139	0.92421	0.9325	0.93521	0.93582

Figure 2. Q2 is an estimate of the predictive ability of the model, and is calculated via cross-validation (CV). In each CV, the predicted data are compared with the original data, and the sum of squared errors is calculated. The prediction error is then summed over all samples (Predicted Residual Sum of Squares or PRESS). For convenience, the PRESS is divided by the initial sum of squares and subtracted from 1 to resemble the scale of the R2. Good predictions will have low PRESS or high Q2.

Metabolites 2021, 11, 296. https://doi.org/10.3390/metabo11050296

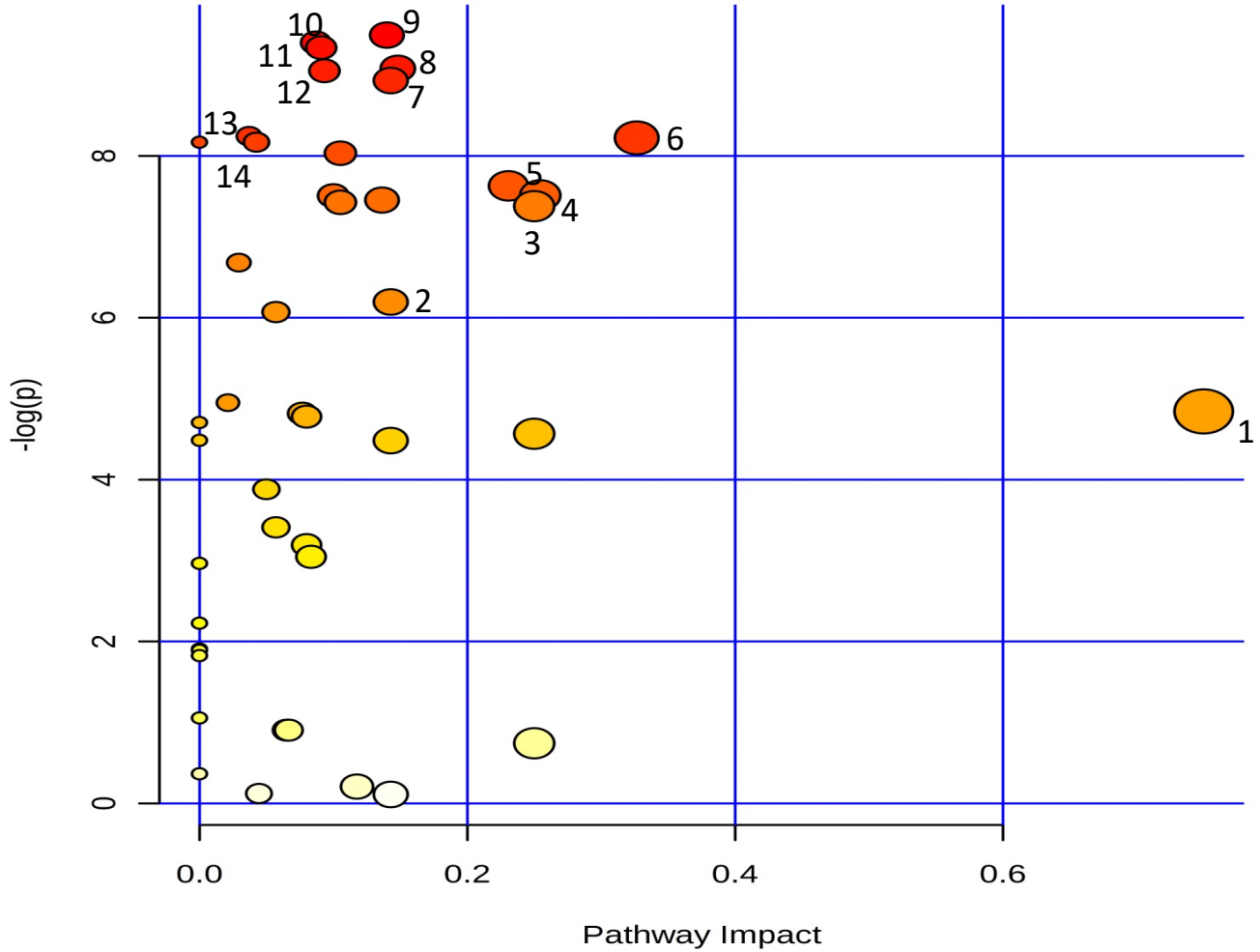

1. Flavone and flavonol biosynthesis
2. Glycerophospholipid metabolism
3. Histidine metabolism
4. Phenylalanine metabolism
5. Phenylpropanoid metabolism
6. Flavonoid biosynthesis
7. Arginine and proline metabolism
8. Amminoacyl-tRNA biosynthesis
9. Glucosinolate biosynthesis
10. Tryptophan metabolism
11. Glutathione metabolism
12. Purine metabolism
13. Glycerolipid metabolism
14. Arginine biosynthesis

Figure 3 . Metabolic Pathway Analysis (MetPA). All the matched pathways are displayed as circles. The colour and size of each circle are based on the *p*-value and pathway impact value, respectively. The graph was obtained by plotting on the *y*-axis the −log of *p* values from the pathway enrichment analysis and on the x-axis the pathway impact values derived from the pathway topology analysis.

Metabolites 2021, 11, 296. https://doi.org/10.3390/metabo11050296

FLAVONOL BIOSYNTHESIS

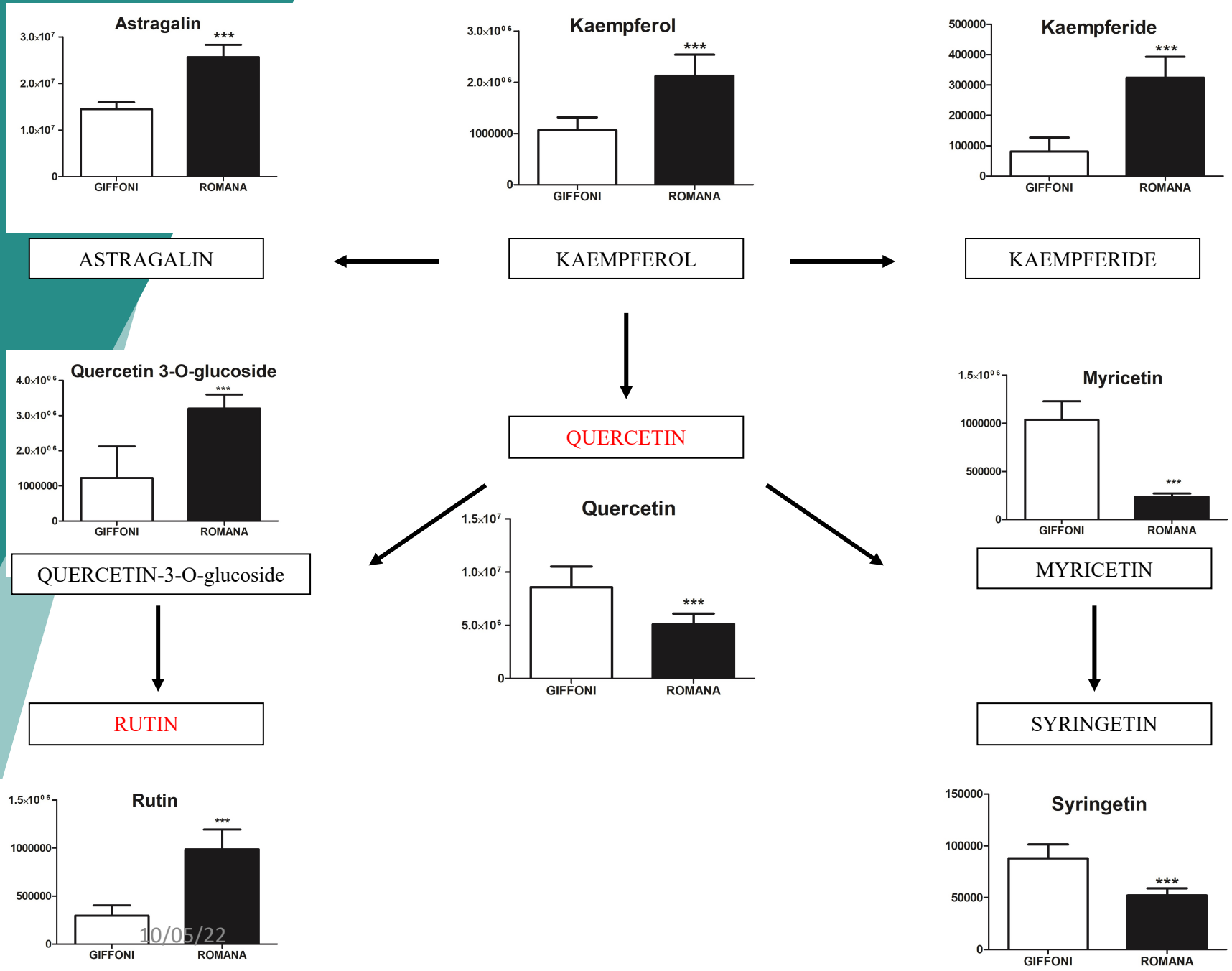

Figure 4 . The level of metabolites involved in the Flavonol biosynthesis were analysed in Giffoni and Romana hazelnut skin. Values are presented as the mean ± SD .* ($P \leq 0,05$) , ** ($P \leq 0,01$).

PHENILPROPANOID BIOSYNTHESIS

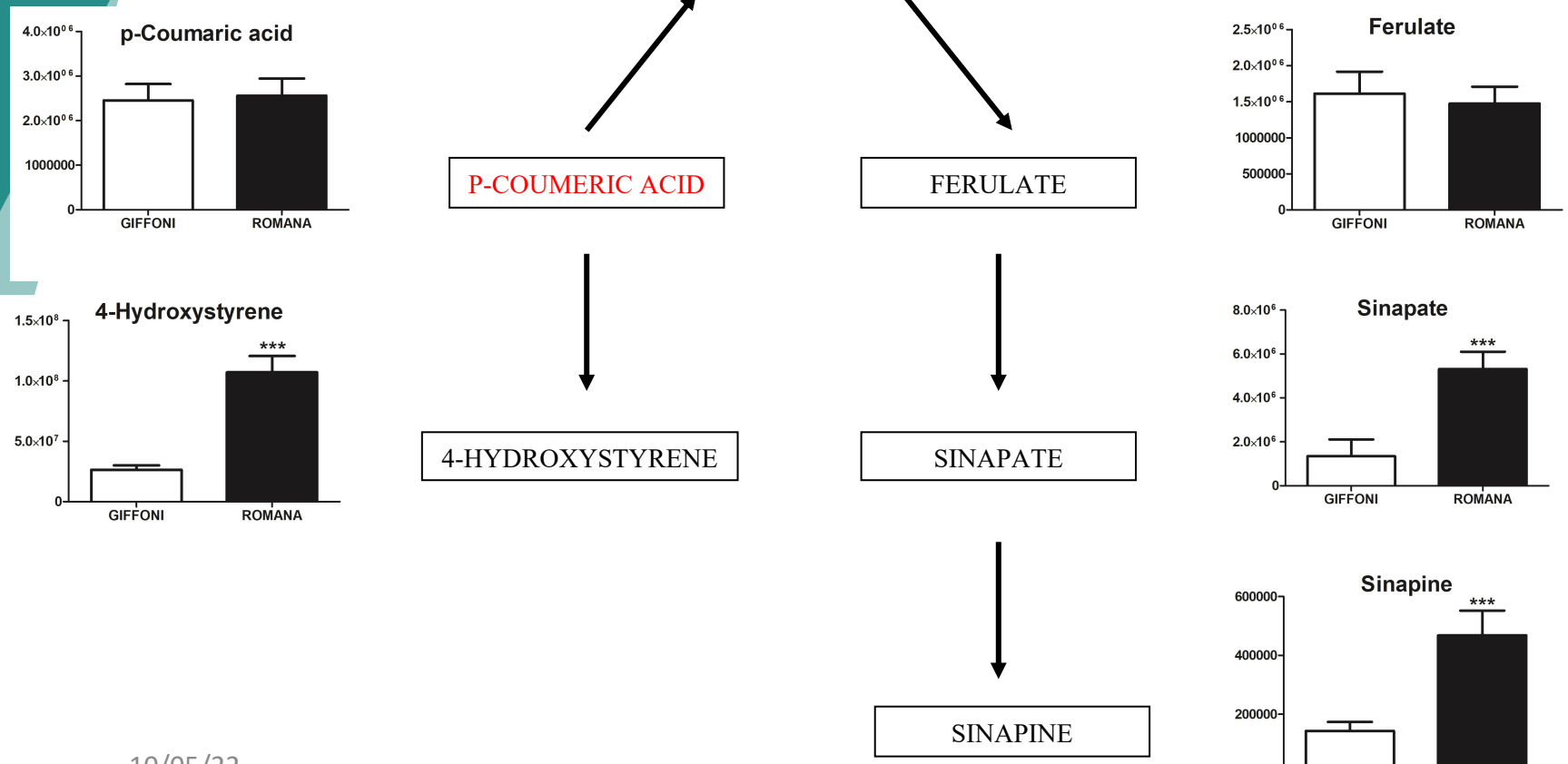

- **Figure 5.** The figure represents metabolites involved in the Phenilpropanoid biosynthesis found in different concentrations in the two varieties of hazelnut skin. Data are presented as the mean ± SD . * ($P \leq 0,05$) , ** ($P \leq 0,01$).

Table 2. List of Phenolic compounds quantified using LC–MS with authentic standards. Data are presented as the mean ± SD.* ($P \leq 0,05$).

Phenolic compounds	Giffoni	Romana
	mg/100g	mg/100g
Quercetin	1.2 ± 0.2*	0.8 ± 0.1
Rutin	0.4 ±0.04	0.7 ± 0.1*
Vitexin	2.3 ± 0.4	3.53 ± 0.7
Caffeic Acid	0.59 ± 0.01	0.65 ± 0.02
Cumaric Acid	0.73 ± 0.03	0.72 ± 0.05